Couple-Stress Effects for the Problem of a Crack Under Concentrated Shear Loading

P.A. GOURGIOTIS , H.G. GEORGIADIS * , M.D. SIFNAIOU

Mechanics Division, National Technical University of Athens,
Zographou, GR-15773, Greece

Abstract: In this paper, we deal with the plane-strain problem of a semi-infinite crack under concentrated loading in an elastic body exhibiting couple-stress effects. The faces of the crack are subjected to a concentrated shear loading at a distance L from the crack tip. This type of loading is chosen since, in principle, shear effects are more pronounced in couple-stress elasticity. The problem involves two characteristic lengths, i.e. the microstructural length ℓ and the distance L between the point of application of the concentrated shear forces and the crack-tip. The presence of this second characteristic length introduces certain difficulties in the mathematical analysis of the problem: a non-standard Wiener-Hopf equation arises, one that contains a forcing term with unbounded behavior at infinity in the transformed plane. Nevertheless, an analytic function method is employed which circumvents the aforementioned difficulty. For comparison purposes, the case of a semi-infinite crack subjected to a distributed shear load is also treated in the present study. Numerical results for the dependence of the stress intensity factor and the energy release rate upon the ratio of the characteristic lengths are presented.

Key Words: Microstructure, micro-mechanics, granular media, generalized continua, couple-stresses, cracks, energy release rate, concentrated loads, integral transforms, analytic functions, Wiener-Hopf technique

---

* Corresponding author. Tel.: +30 210 7721365; fax: +30 210 7721302.
E-mail address: *georgiad@central.ntua.gr (H.G. Georgiadis)*

1. INTRODUCTION

The present work is concerned with the plane-strain problem of a semi-infinite crack in a body with microstructure. The body is acted upon by a pair of concentrated shear forces. The material microstructure is modeled here through the couple-stress theory of elasticity. The standard couple-stress theory (or Cosserat theory with constrained rotations) is the simplest theory in which couple-stresses appear. In particular, couple-stress elasticity assumes that: (i) each material particle has three degrees of freedom, (ii) an augmented form of the Euler-Cauchy principle with a non-vanishing couple traction prevails, and (iii) the strain-energy density depends upon both the strain and the gradient of rotation. Such assumptions are appropriate for materials with granular structure, where the interaction between adjacent elements may introduce internal moments. In this way, characteristic *material lengths* may appear representing the material microstructure. The presence of these material lengths implies that the couple-stress theory encompasses the analytical possibility of size effects, which are absent in the classical theory.

The fundamental concepts of the couple-stress theory were first introduced by Cauchy [1], Voigt [2] and the Cosserat brothers [3], but the subject was generalized and reached maturity only in the 1960s through the studies by Toupin [4], Mindlin and Tiersten [5], and Koiter [6]. Early applications of couple-stress elasticity dealt mainly with stress-concentration problems concerning holes and inclusions (see e.g. [7-9]).

Interesting review articles on couple-stresses and related *generalized continuum theories* were written, e.g., by Lakes [10] and Maugin [11]. In recent years, these theories attracted a renewed and growing interest in dealing with problems of microstructured materials. This is due to the inability of the classical theory to predict the experimentally observed scale effects, and also due to the increasing demands for manufacturing devices at very small scales. Recent examples of successful modeling of microstructure and size effects by the couple-stress theory and related gradient theories include work by, among others, Batra [12], Batra et al. [13], Fleck et al. [14], Vardoulakis and Sulem [15], Huang et al. [16,17], Zhang et al. [18], Lubarda and Markenscoff [19], Georgiadis and Velgaki [20], Georgiadis [21], Radi and Gei [22], Polyzos et al. [23], Lazar and Maugin [24], Grentzelou and Georgiadis [25,26], Georgiadis and Grentzelou [27], Tsamasphyros et al. [28], Giannakopoulos and Stamoulis [29], Gourgiotis and Georgiadis [30], Aravas and Giannakopoulos [31], Gourgiotis et al. [32], and dell'Isola et al. [33].

For materials with microstructure, the characteristic material length mentioned before may be on the same order as the length of the microstructure. For instance, Chen et al. [34] developed a continuum model for cellular materials and found that the continuum description of these materials obey a gradient elasticity theory of the couple-stress type. In the latter study, the intrinsic material length was naturally identified with the cell size. Also, Chang et al. [35] associated the microstructural material constants of the couple-stress theory with the particle size and the inter-particle stiffness in a granular material. In addition, couple-stress theory was successfully utilized in the past to model some materials with microstructure like foams [36] and porous solids [37]. Generally, the couple-stress theory is intended to model situations where a material with microstructure is deformed in *very small* volumes, such as in the immediate vicinity of crack tips, notches, small holes and inclusions, and in micrometer indentations. A recent study by Bigoni and Drugan [38] provides additional references and an interesting account of the determination of couple-stress moduli via homogenization of heterogeneous materials.

Regarding now the subject of the present work, i.e. plane-strain crack problems treated by the couple-stress theory, the first study is due to Sternberg and Muki [39]. They considered the case of a mode I finite-length crack by employing the method of dual integral equations. In their work, only asymptotic results were obtained showing that both stress and couple-stress fields exhibit a square-root singularity, while the rotation field is bounded at the crack-tip. Later on, Atkinson and Leppington [40] studied the problem of a semi-infinite crack by using the Wiener-Hopf technique. More recently, Huang et al. [16] using the method of eigenfunction expansions, provided near-tip asymptotic fields for mode I and mode II crack problems in couple-stress elasticity. Also, Huang et al. [17] using the Wiener-Hopf technique obtained full-field solutions for semi-infinite cracks under in-plane remote loading in elastic-plastic materials with strain-gradient effects of the couple-stress type. Recently, Gourgiotis and Georgiadis [41,42] extended the distributed dislocation technique in studying finite-length crack problems within the context of couple-stress elasticity. The crack problems were modeled by a continuous distribution of dislocations and disclinations that created both standard stresses and couple stresses in the body. In particular, it was shown that the mode I crack problem was governed by a coupled system of singular integral equations with both Cauchy-type and logarithmic kernels, whereas the mode II case was governed by a singular integral equation with a more complicated kernel than that in classical elasticity. The results showed that the stress intensity factor is appreciably higher than the one predicted by classical elasticity (stress aggravation effect). It was also shown that the J-integral (energy release rate) in couple-stress elasticity tends continuously to its counterpart in classical elasticity as $\ell/a \to 0$, where a is the half of the crack

length and ℓ is the characteristic material length. For $\ell \neq 0$, a *decrease* in the values of the energy release rate is noticed as compared to the ones given by the classical theory. Finally, we mention that related analytical studies, within the context of the more general theory of dipolar gradient elasticity (i.e. a theory that includes both rotation and stretch gradients), were carried out by Shi et al. [43] and Gourgiotis and Georgiadis [30]. In particular, Shi et al. [43] using the Wiener-Hopf technique investigated the elastic problem of a *semi-infinite* crack in a incompressible material by considering a gradient theory, which is the limit of a gradient plasticity theory [44] with the plastic work hardening exponent $n=1$. Also, Gourgiotis and Georgiadis [30] employing the method of hypersingular integral equations studied the problem of a *finite-length* crack in a microstructured solid under remotely applied plane-strain loadings, and examined the effect of Poisson's ratio in the solution and the ratio of the crack length over the pertinent material length. In both cases the results showed significant departure from the predictions of classical elasticity and couple-stress elasticity. Indeed, it was shown that the stresses are compressive ahead of the crack-tip exhibiting a cohesive character. Moreover, in the vicinity of the crack tip, the crack-face displacement closes more smoothly as compared to the standard result and the strain field is bounded. Similar results were obtained using finite elements by Chen et al. [45] and Wei [46] in the theory of phenomenological strain gradient plasticity, and more recently by Aravas and Giannakopoulos [31] in dipolar gradient elasticity.

In the present study, which is closely allied in scope to [41,42], we examine the plane-strain response of a body with couple-stress effects containing a semi-infinite crack subjected to a pair of equal, but opposite, concentrated shear forces. This type of loading is chosen since, in general, *shear effects* are more pronounced when couple-stresses are taken into account. In fact, this behavior can be justified from the fact that couple-stress elasticity is based only on the gradient of the rotation, and does not include stretch gradients; hence the couple-stress effects are more intense in the antisymmetric modes of deformation for crack and notch problems. Indeed, as it has been observed in [17,41,42], the increase of the stress intensity factor in the mode II case, with respect to the classical K field, is always higher than the respective increase in the mode I case. Moreover, in a recent work, Gourgiotis and Georgiadis [47] showed that in the general notch problem the strength of the singularity associated with the antisymmetric loading is always stronger than that for the symmetric loading. These findings also corroborate this behavior. The present boundary value problem involves both load-induced and geometrically-induced concentrations of stress. The former stress concentration is due to the presence of the concentrated load, while the latter is due to the presence of the crack. In addition, the problem involves two characteristic lengths, i.e. the microstructural length ℓ and the distance L between the point of application of the concentrated

loading and the crack-tip. It is well-known that the second characteristic length introduces a certain mathematical difficulty in the course of obtaining an analytical solution through the Wiener-Hopf technique. In particular, it gives rise to a non-standard functional equation in the Laplace transform domain that contains a term with an exponentially unbounded behavior at infinity. This situation is treated here by following a technique proposed by Georgiadis and Brock [48] that is based on the exact solution of a functional equation through contour integration and analytic-continuation arguments. Finally, in addition to the concentrated load case, we also treat the problem of a semi-infinite crack subjected to distributed shear tractions. This was done for the purpose of comparing results for the variation of J-integral with the previous case of a crack under concentrated loading and also for the purpose of completeness. In order to avoid an unbounded behavior of the solution (recall that a semi-infinite crack is involved), the distributed shear tractions are taken to be exponentially decaying from the crack tip (and not to be uniform along the crack faces).

We notice that the results obtained in the concentrated load case differ in some respects from previous results concerning finite-length [41,42] or semi-infinite [17,40] cracks under remote or distributed (along the crack-faces) loadings. In particular, the ratio $J/J^{clas.}$ (where $J^{clas.}$ is the energy release rate for the same problem treated by classical elasticity) initially increases (from unity corresponding to the limit $\ell/L \to 0$) with increasing values of ℓ/L and after reaching a bounded maximum only then it decreases to values less than unity. Recall that in the other cases treated before, the ratio $J/J^{clas.}$ decreases monotonically to values less than unity with increasing values of ℓ/a, where a is the half of the crack length. On the other hand, the stress intensity factor K_{II} is significantly higher than the one predicted by classical elasticity. However, unlike the cases treated in [40-42], the ratio $K_{II}/K_{II}^{clas.}$ does not decrease monotonically with increasing values of ℓ/L. On the contrary, it exhibits a bounded maximum when the material microstructure becomes comparable with the geometric length L.

2. FUNDAMENTALS OF COUPLE-STRESS ELASTICITY

In this Section, we will give a brief account of the theory of standard couple-stress elasticity. More detailed presentations can be found in [5-6]. Interesting presentations of the theory can also be found in the works by Aero and Kuvshinskii [49], Palmov [50], and Muki and Sternberg [51]. The basic equations of dynamical couple-stress theory (including the effects of micro-inertia) were given

by Georgiadis and Velgaki [20], who also provided estimates for the couple-stress modulus (in plane problems) in terms of the size of the unit cube in granular materials.

As mentioned before, couple-stress elasticity assumes that: (i) each material particle has three degrees of freedom, (ii) an augmented form of the Euler-Cauchy principle with a non-vanishing couple traction prevails, and (iii) the strain-energy density depends upon both strain and the gradient of rotation.

In the absence of inertia effects, for a control volume CV with bounding surface S, the balance laws for the linear and angular momentum read

$$\iint_S T_q^{(n)}\, dS + \iiint_{CV} F_q\, d\left(CV\right) = 0 \quad , \tag{1}$$

$$\iint_S \left(e_{qpk} x_p\, T_k^{(n)} + M_q^{(n)}\right)\, dS + \iiint_{CV} \left(e_{qpk} x_p\, F_k + C_q\right)\, d\left(CV\right) = 0 \quad , \tag{2}$$

where a Cartesian rectangular coordinate system $Ox_1x_2x_3$ is used along with indicial notation and summation convention, e_{qpk} is the Levi-Civita alternating symbol, $T_q^{(n)}$ is the surface force per unit area, F_q is the body force per unit volume, $M_q^{(n)}$ is the surface moment per unit area, C_q is the body moment per unit volume, and x_p designate the components of the position vector of each material particle with elementary volume $d\left(CV\right)$.

Next, pertinent *force-stress* and *couple-stress* tensors are introduced by considering the equilibrium of the elementary material tetrahedron and enforcing (1) and (2), respectively. The force stress tensor σ_{pq} (which is asymmetric) is then defined by

$$T_q^{(n)} = \sigma_{pq} n_p \quad , \tag{3}$$

and the couple-stress tensor μ_{pq} (which is also asymmetric) by

$$M_q^{(n)} = \mu_{pq} n_p \quad , \tag{4}$$

where n_p are the direction cosines of the outward unit vector $\mathbf{n}$, which is normal to the surface. In addition, just like the third Newton's law $\mathbf{T^{(n)}} = -\mathbf{T^{(-n)}}$ is proved to hold by considering the

equilibrium of a material 'slice', it can also be proved that $\mathbf{M}^{(\mathbf{n})} = -\mathbf{M}^{(-\mathbf{n})}$ (see e.g. [52]). The couple-stresses μ_{pq} are expressed in dimensions of [force][length]$^{-1}$. Further, σ_{pq} can be decomposed into its symmetric and anti-symmetric components as follows

$$\sigma_{pq} = \tau_{pq} + \alpha_{pq} \quad , \tag{5}$$

with $\tau_{pq} = \tau_{qp}$ and $\alpha_{pq} = -\alpha_{qp}$, whereas it is advantageous to decompose μ_{pq} into its deviatoric $\mu_{pq}^{(D)}$ and spherical $\mu_{pq}^{(S)}$ parts in the following manner

$$\mu_{pq} = m_{pq} + \frac{1}{3}\delta_{pq}\mu_{kk} \quad , \tag{6}$$

where $\mu_{pq}^{(D)} = m_{pq}$, $\mu_{pq}^{(S)} = (1/3)\delta_{pq}\mu_{kk}$, and δ_{pq} is the Kronecker delta. Now, with the above definitions and the help of the Green-Gauss theorem, one may obtain the stress equations of motion. Equation (2) leads to the following moment equation

$$\partial_p \mu_{pq} + e_{pqk}\sigma_{kp} + C_q = 0 \ , \tag{7}$$

which can also be written as

$$\frac{1}{2}e_{pqk}\partial_l \mu_{lk} + \alpha_{pq} + \frac{1}{2}e_{pqk}C_k = 0 \quad . \tag{8}$$

where $\partial_p(\ ) \equiv \partial(\ )/\partial x_p$. Note from Eqs. (7) and (8) that the stress tensor σ_{pq} is symmetric in the absence of couple-stresses and body couples.

Also, Eq. (1) leads to the following force equation

$$\partial_p \sigma_{pq} + F_q = 0 \quad , \tag{9}$$

or, by virtue of (5), to the following equation

$$\partial_p \tau_{pq} + \partial_p \alpha_{pq} + F_q = 0 \quad . \tag{10}$$

Further, combining (8) and (10) yields the single equation

$$\partial_p \tau_{pq} - \frac{1}{2} e_{pqk} \partial_p \partial_l \mu_{lk} + F_q - \frac{1}{2} e_{pqk} \partial_p C_k = 0 \quad . \tag{11}$$

Finally, in view of (6) and by taking into account that $\mathrm{curl}\left(\mathrm{div}\left((1/3)\,\delta_{pq}\mu_{kk}\right)\right) = 0$, we write (11) as

$$\partial_p \tau_{pq} - \frac{1}{2} e_{pqk} \partial_p \partial_l m_{lk} + F_q - \frac{1}{2} e_{pqk} \partial_p C_k = 0 \quad , \tag{12}$$

which is the final *equation of equilibrium*.

For the kinematical description of the continuum, the following quantities are defined in the framework of the geometrically linear theory

$$\varepsilon_{pq} = \frac{1}{2}\left(\partial_p u_q + \partial_q u_p\right) \quad , \tag{13}$$

$$\omega_{pq} = \frac{1}{2}\left(\partial_p u_q - \partial_q u_p\right) \quad , \tag{14}$$

$$\omega_q = \frac{1}{2} e_{qpk} \partial_p u_k \quad , \tag{15}$$

$$\kappa_{pq} = \partial_p \omega_q \quad , \tag{16}$$

where ε_{pq} is the strain tensor, ω_{pq} is the rotation tensor, ω_q is the rotation vector, and κ_{pq} is the curvature tensor (i.e. the gradient of rotation or the curl of the strain) expressed in dimensions of [length]$^{-1}$. Notice also that Eq. (16) can alternatively be written as

$$\kappa_{pq} = \frac{1}{2} e_{qlk} \partial_p \partial_l u_k = e_{qlk} \partial_l \varepsilon_{pk} \quad . \tag{17}$$

Equation (17) expresses compatibility for curvature and strain fields. The compatibility equations for the strain components are the usual Saint Venant's compatibility equations. Further, the identity

$\partial_k \kappa_{pq} = \partial_k \partial_p \omega_q = \partial_p \kappa_{kq}$ defines the compatibility equations for the curvature components. We notice also that $\kappa_{pp} = 0$ because $\kappa_{pp} = \partial_p \omega_p = (1/2) e_{pqk} u_{k,qp} = 0$ and, therefore, κ_{pq} has only eight independent components. The tensor κ_{pq} is obviously an asymmetric tensor.

The traction boundary conditions, at any point on a smooth boundary or section, consist of the following three *reduced* force-tractions and two *tangential* couple-tractions [5,6]

$$P_q^{(n)} = \sigma_{pq} n_p - \frac{1}{2} e_{qpk} n_p \partial_k m_{(nn)} \ , \tag{18}$$

$$R_q^{(n)} = m_{pq} n_p - m_{(nn)} n_q \ , \tag{19}$$

where $m_{(nn)} = n_p n_q m_{pq}$ is the normal component of the deviatoric couple-stress tensor m_{pq}. It should be noted that in the case in which edges appear along the boundary an additional boundary condition should be imposed. Indeed, as Koiter [6] pointed out, a force (per unit length) *tangential* to the edge should be specified according to the relation: $Q = (1/2) [\![m_{(nn)}]\!]$, where $[\![\ ]\!]$ denotes the jump of the enclosed quantity through the edge. This tangential line load along the edge is the counterpart of the concentrated normal force which may be specified at the corner of the edge of a plate or shell.

It is worth noticing that at first sight, it might seem plausible that the surface tractions (i.e. the force-traction and the couple-traction) can be prescribed arbitrarily on the external surface of the body through relations (3) and (4), which stem from the equilibrium of the material tetrahedron. However, as was pointed out by in [6], the resulting number of six traction boundary conditions (three force-tractions and three couple-tractions) would be in contrast with the *five* geometric boundary conditions that can be imposed. Indeed, since the rotation vector ω_q in couple-stress elasticity is not independent of the displacement vector u_q (as (15) suggests), the normal component of the rotation is fully specified by the distribution of tangential displacements over the boundary. Therefore, only the three displacement and the two tangential rotation components can be prescribed independently. As a consequence, only *five* surface tractions (i.e. the work conjugates of the above five independent kinematical quantities) can be specified at a point of the bounding surface of the body, i.e. Eqs. (18) and (19). On the contrary, in the Cosserat (micropolar) theory, the traction boundary conditions are six since the rotation is fully independent of the displacement vector (see e.g. [53]). In the latter case, the tractions can directly be derived from the equilibrium of the material tetrahedron, so (3) and (4) are the pertinent traction boundary conditions.

For a linear and isotropic material behavior, the strain-energy density has the following form

$$W \equiv W\left(\varepsilon_{pq},\kappa_{pq}\right)=\frac{1}{2}\lambda\varepsilon_{pp}\varepsilon_{qq}+\mu\varepsilon_{pq}\varepsilon_{pq}+2\eta\kappa_{pq}\kappa_{pq}+2\eta'\kappa_{pq}\kappa_{qp}\ , \tag{20}$$

where $\left(\lambda,\mu,\eta,\eta'\right)$ are material constants. Then, Eq. (20) leads, through the standard variational manner, to the following constitutive equations

$$\tau_{pq}\equiv\sigma_{(pq)}=\frac{\partial W}{\partial\varepsilon_{pq}}=\lambda\delta_{pq}\varepsilon_{kk}+2\mu\varepsilon_{pq}\ , \tag{21}$$

$$m_{pq}=\frac{\partial W}{\partial\kappa_{pq}}=4\eta\kappa_{pq}+4\eta'\kappa_{qp}\ . \tag{22}$$

In view of (21) and (22), the moduli $\left(\lambda,\mu\right)$ have the same meaning as the Lamé constants of classical elasticity theory and are expressed in dimensions of [force][length]$^{-2}$, whereas the moduli $\left(\eta,\eta'\right)$ account for couple-stress effects and are expressed in dimensions of [force]. Further, following Mindlin and Tiersten [5], we assume W to be a positive definite function of its arguments, so that

$$3\lambda+2\mu>0\ ,\quad \mu>0\ ,\quad \eta>0\ ,\quad -1<\frac{\eta'}{\eta}<1\ . \tag{23a-d}$$

Incorporating now the constitutive relations (21) and (22) into the equation of equilibrium (12) and using the geometric relations (13)-(16), one may obtain the displacement equations of equilibrium [6]

$$\nabla^2\mathbf{u}-\ell^2\nabla^4\mathbf{u}+\boldsymbol{\nabla}\left[\left(1-2\nu\right)^{-1}\left(\boldsymbol{\nabla}\cdot\mathbf{u}\right)+\ell^2\nabla^2\left(\boldsymbol{\nabla}\cdot\mathbf{u}\right)\right]=0\ , \tag{24}$$

where ν is the Poisson's ratio, $\ell\equiv\left(\eta/\mu\right)^{1/2}$ is a characteristic material length, and the absence of body forces and couples is assumed. In the limit $\ell\to 0$, the Navier-Cauchy equations of classical linear isotropic elasticity are recovered from (24). Indeed, the fact that Eqs. (24) have an increased order w.r.t. their limit case (recall that the Navier-Cauchy equations are PDEs of the second order)

and the coefficient ℓ multiplies the higher-order term reveals the *singular-perturbation* character of the couple-stress theory and the emergence of associated *boundary-layer* effects. Moreover, applying the gradient and the curl operator to Eq. (24), we obtain the following relations for the dilatation and the rotation, respectively

$$\nabla^2 e = 0 \ , \ \left(1-\ell^2\nabla^2\right)\nabla^2\boldsymbol{\omega} = 0 \ , \tag{25a,b}$$

where $e \equiv \boldsymbol{\nabla}\cdot\mathbf{u}$ is the dilatation (volumetric strain). Thus, we observe that the dilatation is governed by the same equation as in classical elasticity. We also note that (25a) is of the second order, whereas each equation in (24) is of the fourth order. As Koiter [6] pointed out, this fact reconciles the order of the elliptic system (24) with the number of five boundary conditions.

Finally, the following points are of notice: (i) Since $\kappa_{pp} = 0$, $m_{pp} = 0$ is also valid and therefore the tensor m_{pq} has only eight independent components. (ii) The spherical part of the couple-stress tensor $(1/3)\,\mu_{kk}\,\delta_{pq}$ does not appear in the final equation of equilibrium, nor in the reduced boundary conditions and the constitutive equations. Consequently, μ_{kk} and the antisymmetric part of the stress tensor α_{pq} are left indeterminate within the couple-stress theory. It is noted that the latter quantities are related by the following equation

$$\alpha_{pq} = e_{lqp}\left(\eta\, e_{lmn}u_{n,mkk} + (1/6)\,\mu_{kk,l}\right) \ , \tag{26}$$

which is a consequence of (8) in the absence of body couples. However, the aforementioned inherent indeterminacy of the couple-stress theory is removed if we adopt the normalization $\mu_{kk} = 0$. Accordingly, this condition assures the continuous transition form couple-stress theory to the classical theory [51].

3. BASIC EQUATIONS IN PLANE-STRAIN

For a body that occupies a domain in the (x, y)-plane under conditions of plane strain, the displacement field takes the general form

$$u_x \equiv u_x(x,y) \neq 0 \ , \qquad u_y \equiv u_y(x,y) \neq 0 \ , \qquad u_z \equiv 0 \ . \tag{27a-c}$$

Further, Muki and Sternberg [51] showed that, if the general 3D equations of Section 2 are combined with the restrictions in (27) and the normalization $\mu_{kk} = 0$ of the couple-stress field is adopted, all field quantities are independent upon the coordinate z. Accordingly, except for $\omega_z \equiv \omega$ and $(\kappa_{xz}, \kappa_{yz})$, all other components of the rotation vector and the curvature tensor vanish identically in the particular case of plane-strain considered here. The non-vanishing components of the stress and couple-stress tensors are derived from (21) and (22). Vanishing body forces and body couples are assumed in what follows. In view of the above, the following kinematic relations are obtained

$$\varepsilon_{xx} = \partial_x u_x \ , \quad \varepsilon_{yy} = \partial_y u_y \ , \quad \varepsilon_{xy} = \varepsilon_{yx} = (1/2)\left(\partial_x u_y + \partial_y u_x\right) \ , \tag{28a-c}$$

$$\omega = (1/2)\left(\partial_x u_y - \partial_y u_x\right) \ , \quad \kappa_{xz} = \partial_x \omega \ , \quad \kappa_{yz} = \partial_y \omega \ , \tag{29a-c}$$

whereas the constitutive equations furnish

$$\varepsilon_{xx} = (2\mu)^{-1}\left[\ \tau_{xx} - \nu\left(\tau_{xx} + \tau_{yy}\right)\right] \ , \ \varepsilon_{yy} = (2\mu)^{-1}\left[\ \tau_{yy} - \nu\left(\tau_{xx} + \tau_{yy}\right)\right] \ ,$$

$$\varepsilon_{xy} = (2\mu)^{-1}\,\tau_{xy} \quad , \tag{30a-c}$$

$$\kappa_{xz} = \left(4\mu\ell^2\right)^{-1} m_{xz} \ , \quad \kappa_{yz} = \left(4\mu\ell^2\right)^{-1} m_{yz} \ . \tag{31a,b}$$

Accordingly, the equations of equilibrium (7) and (9) in the present circumstances reduce to

$$\frac{\partial \sigma_{xx}}{\partial x} + \frac{\partial \sigma_{yx}}{\partial y} = 0 \ , \qquad \frac{\partial \sigma_{xy}}{\partial x} + \frac{\partial \sigma_{yy}}{\partial y} = 0 \ , \tag{32a,b}$$

$$\sigma_{xy} - \sigma_{yx} + \frac{\partial m_{xz}}{\partial x} + \frac{\partial m_{yz}}{\partial y} = 0 \ . \tag{33}$$

Moreover, the compatibility equations for curvature and strain fields in conjunction with (30)-(33) lead to the following stress and couple-stress equations of compatibility [7]

$$\frac{\partial^2 \sigma_{xx}}{\partial y^2} - \frac{\partial^2}{\partial x \partial y}\left(\sigma_{xy} + \sigma_{yx}\right) + \frac{\partial^2 \sigma_{yy}}{\partial x^2} = \nu \nabla^2 \left(\sigma_{xx} + \sigma_{yy}\right) , \tag{34}$$

$$\frac{\partial m_{xz}}{\partial y} = \frac{\partial m_{yz}}{\partial x} , \tag{35}$$

$$m_{xz} = -2\ell^2 \frac{\partial}{\partial y}\left[\sigma_{xx} - \nu\left(\sigma_{xx} + \sigma_{yy}\right)\right] + \ell^2 \frac{\partial}{\partial x}\left(\sigma_{xy} + \sigma_{yx}\right) , \tag{36}$$

$$m_{yz} = 2\ell^2 \frac{\partial}{\partial x}\left[\sigma_{yy} - \nu\left(\sigma_{xx} + \sigma_{yy}\right)\right] - \ell^2 \frac{\partial}{\partial y}\left(\sigma_{xy} + \sigma_{yx}\right) . \tag{37}$$

Note that only three of the four equations of compatibility are independent. Indeed, Eqs. (35)-(37) imply (34), while Eqs. (34), (36) and (37) yield (35) [7,51].

Next, regarding the traction boundary conditions in the plane strain case, we note that these are defined through Eqs. (18) and (19) by taking also into account that the normal component of the couple-stress $m_{(nn)}$ is zero. Indeed, since the components $(m_{xx}, m_{xy}, m_{yx}, m_{yy})$ of the couple-stress tensor vanish identically in the plane strain case (recall that in this case, all field quantities are independent upon the coordinate z), we conclude that $m_{(nn)} \equiv n_p n_q m_{pq} = 0$. This, in turn, implies that no edge forces: $Q = (1/2)\left[\!\left[m_{(nn)} \right]\!\right]$ appear at the corners of a boundary or section in plane strain. However, we remark that these edge forces should be considered in antiplane strain problems where, in general, $m_{(nn)} \neq 0$. Also, pertinent edge conditions should be taken into account in both plane and antiplane strain cases, in the more general theory of dipolar gradient elasticity (Gourgiotis et al. [32], Sciarra and Vidoli [54]).

Finally, Mindlin [7] introduced pertinent *stress functions* (generalizing the Airy stress function of classical elasticity) by showing that the complete solution of Eqs. (32), (33) and (35) admits the following representation

$$\sigma_{xx} = \frac{\partial^2 \Phi}{\partial y^2} - \frac{\partial^2 \Psi}{\partial x \partial y} , \quad \sigma_{yy} = \frac{\partial^2 \Phi}{\partial x^2} + \frac{\partial^2 \Psi}{\partial x \partial y} ,$$

$$\sigma_{xy} = -\frac{\partial^2 \Phi}{\partial x \partial y} - \frac{\partial^2 \Psi}{\partial y^2} , \; \sigma_{yx} = -\frac{\partial^2 \Phi}{\partial x \partial y} + \frac{\partial^2 \Psi}{\partial x^2} , \tag{38a-d}$$

$$m_{xz} = \frac{\partial \Psi}{\partial x} , \quad m_{yz} = \frac{\partial \Psi}{\partial y} , \tag{39a,b}$$

where $\Phi \equiv \Phi(x,y)$ and $\Psi \equiv \Psi(x,y)$ are two arbitrary but sufficiently smooth functions. Further, substitution of (38) and (39) into (36) and (37) results in the following pair of differential equations, for the stress functions

$$\frac{\partial}{\partial x}\left(\Psi - \ell^2\nabla^2\Psi\right) = -2(1-\nu)\ell^2\nabla^2\left(\frac{\partial \Phi}{\partial y}\right), \tag{40}$$

$$\frac{\partial}{\partial y}\left(\Psi - \ell^2\nabla^2\Psi\right) = 2(1-\nu)\ell^2\nabla^2\left(\frac{\partial \Phi}{\partial x}\right), \tag{41}$$

which then lead to the uncoupled PDEs

$$\nabla^4\Phi = 0, \tag{42}$$

$$\nabla^2\Psi - \ell^2\nabla^4\Psi = 0\ . \tag{43}$$

As the quantities ℓ, $\partial_x\Psi$, and $\partial_y\Psi$ tend to zero, the above representation passes over into Airy's representation.

In addition, from (28)-(33) and (38)-(39), one can obtain the following relations connecting the displacement field and Mindlin's stress functions

$$\frac{\partial u_x}{\partial x} = \frac{1}{2\mu}\left(\frac{\partial^2\Phi}{\partial y^2} - \frac{\partial^2\Psi}{\partial x\partial y} - \nu\nabla^2\Phi\right), \qquad \frac{\partial u_y}{\partial y} = \frac{1}{2\mu}\left(\frac{\partial^2\Phi}{\partial x^2} + \frac{\partial^2\Psi}{\partial x\partial y} - \nu\nabla^2\Phi\right),$$

$$\frac{\partial u_x}{\partial y} + \frac{\partial u_y}{\partial x} = -\frac{1}{2\mu}\left(2\frac{\partial^2\Phi}{\partial x\partial y} - \frac{\partial^2\Psi}{\partial x^2} + \frac{\partial^2\Psi}{\partial y^2}\right). \tag{44a-c}$$

4. FORMULATION OF THE CRACK PROBLEM

Consider now a semi-infinite crack in a body of infinite extent under plane strain conditions. The body is governed by the equations of couple-stress elasticity. A Cartesian coordinate system $Oxyz$ is attached to the cracked body with the origin at the crack tip (see Fig. 1). The crack lies in the plane $(-\infty < x < 0,\ y = 0)$ and is sheared by a pair of concentrated line loads $\pm S$ at $x = -L$. These

loads have dimensions of [force][length]$^{-1}$. The crack faces are considered traction free, except for the point of application of the concentrated forces.

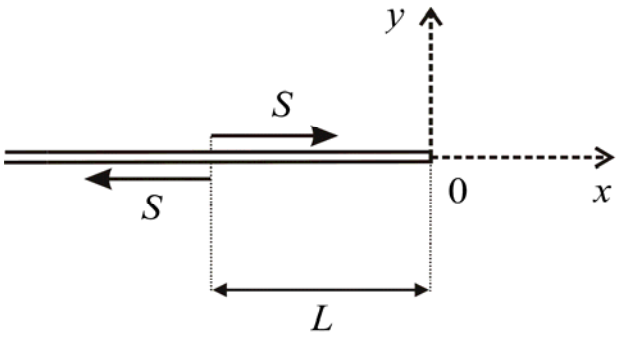

Figure 1. Semi-infinite crack under the action of a pair of concentrated shear forces.

Because of anti-symmetry with respect to the plane $y=0$, the problem can be viewed as a half-plane problem in the region $\left(-\infty<x<\infty,\ 0\le y<\infty\right)$ under the following boundary conditions

$$\sigma_{yx}\left(y=0\right)=-S\delta\left(x+L\right) \quad \text{for} \quad -\infty<x<0\ , \tag{45}$$

$$\sigma_{yy}\left(y=0\right)=0 \quad \text{for} \quad -\infty<x<\infty\ , \tag{46}$$

$$m_{yz}\left(y=0\right)=0 \quad \text{for} \quad -\infty<x<\infty\ , \tag{47}$$

$$u_{x}\left(y=0\right)=0 \quad \text{for} \quad 0<x<\infty\ , \tag{48}$$

where $\delta(\ )$ is the Dirac delta distribution with 'dimensions' of $(\ )^{-1}$.

An exact solution of the boundary value problem described above will be obtained here through two-sided Laplace transforms [55,56], and a variant of the Wiener-Hopf technique [48]. The direct and inverse two-sided Laplace transforms (which are equivalent to the standard Fourier transforms) are defined as

$$f^{*}\left(p,y\right)=\int_{-\infty}^{\infty}f\left(x,y\right)e^{-px}dx\ , \tag{49a}$$

$$f(x,y)=\frac{1}{2\pi \mathrm{i}}\int_{Br} f^*(p,y)e^{px}dp \ , \tag{49b}$$

where Br denotes the Bromwich inversion path within the region of analyticity of the function $f^*(p,y)$ in the complex p-plane. Transforming the field equations (42) and (43) with (49a), we obtain the following ODEs

$$\frac{d^4\Phi^*(p,y)}{dy^4}+2p^2\frac{d^2\Phi^*(p,y)}{dy^2}+p^4\Phi^*(p,y)=0 \ , \tag{50}$$

$$\ell^2\frac{d^4\Psi^*(p,y)}{dy^4}+\left(2\ell^2p^2-1\right)\frac{d^2\Psi^*(p,y)}{dy^2}+\left(\ell^2p^4-p^2\right)\Psi^*(p,y)=0 \ . \tag{51}$$

The above equations have the following general solutions that will be required to be *bounded* as $y\to+\infty$

$$\Phi^*(p,y)=\left[A(p)+yD(p)\right]e^{-\beta y} \ , \tag{52}$$

$$\Psi^*(p,y)=B(p)e^{-\beta y}+C(p)e^{-\gamma y} \ , \tag{53}$$

where $A(p)$, $B(p)$, $C(p)$ and $D(p)$ are yet unknown functions, $\beta\equiv\beta(p)=\left(\varepsilon^2-p^2\right)^{1/2}$ with ε being a real number such that $\varepsilon\to 0^+$, and $\gamma\equiv\gamma(p)=\left(a^2-p^2\right)^{1/2}$ with $a\equiv(1/\ell)$. In fact, introducing ε facilitates the introduction of the branch cuts for $\beta=\left(-p^2\right)^{1/2}$ (see e.g. [21,58]). Now, for the solution to be bounded as $y\to+\infty$, the p-plane should be cut in the way shown in Fig. 2. This introduction of branch cuts secures that the functions (β,γ) are single-valued and that $\mathrm{Re}(\beta)>0$ and $\mathrm{Re}(\gamma)>0$ along the Bromwich path.

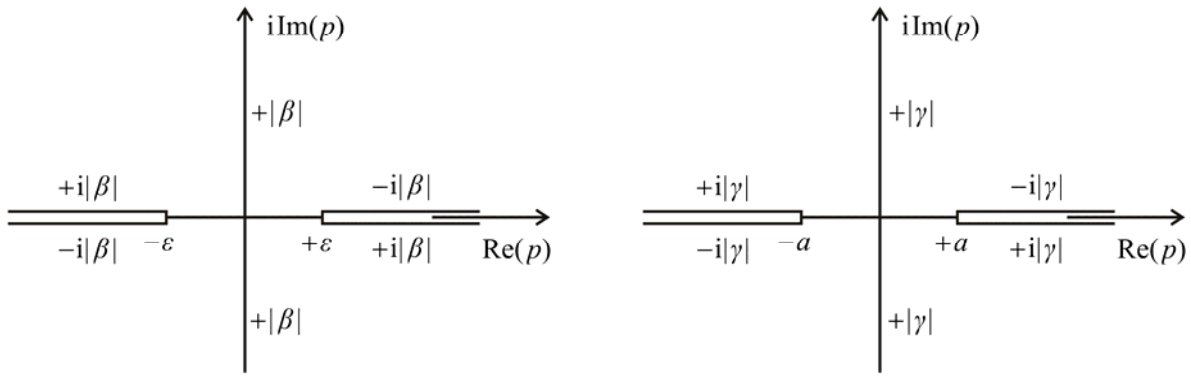

Figure 2. Branch cuts for the functions $\beta(p)$ and $\gamma(p)$.

The transformed stresses and couple-stresses can now be written in terms of the transformed stress functions Φ^* and Ψ^* as follows

$$\sigma_{xx}^* = \frac{d^2\Phi^*}{dy^2} - p\frac{d\Psi^*}{dy}\ , \qquad \sigma_{xy}^* = -p\frac{d\Phi^*}{dy} - \frac{d^2\Psi^*}{dy^2}\ ,$$

$$\sigma_{yx}^* = -p\frac{d\Phi^*}{dy} + p^2\Psi^*\ , \qquad \sigma_{yy}^* = p^2\Phi^* + p\frac{d\Psi^*}{dy}\ , \tag{54a-d}$$

$$m_{xz}^* = p\,\Psi^*\ , \qquad m_{yz}^* = \frac{d\Psi^*}{dy}\ , \tag{55a,b}$$

while the displacements in (44) furnish in the transform domain

$$2\mu u_x^* = \frac{1}{p}\left[(1-\nu)\frac{d^2\Phi^*}{dy^2} - \nu\, p^2\Phi^* - p\frac{d\Psi^*}{dy}\right], \tag{56a}$$

$$2\mu u_y^* = \frac{1}{p^2}\left[-(1-\nu)\frac{d^3\Phi^*}{dy^3} - (2-\nu)p^2\frac{d\Phi^*}{dy} + p^3\Psi^*\right]. \tag{56b}$$

In view of the above, the transformed expressions for the stresses and displacements that enter the boundary conditions take the following form

$$\sigma_{yx}^{*}\left(p,y\right)=p\left(\beta A+\beta yD-D\right)e^{-\beta y}+p^{2}\left(Be^{-\beta y}+Ce^{-\gamma y}\right)\ , \tag{57}$$

$$\sigma_{yy}^{*}\left(p,y\right)=p^{2}\left(A+yD\right)e^{-\beta y}-p\left(\beta Be^{-\beta y}+\gamma Ce^{-\gamma y}\right)\ , \tag{58}$$

$$m_{yz}^{*}\left(p,y\right)=-\beta Be^{-\beta y}-\gamma Ce^{-\gamma y}\ , \tag{59}$$

$$2\mu u_{x}^{*}\left(p,y\right)=-p\left(A+yD\right)e^{-\beta y}+\beta\left(B-2\left(1-\nu\right)D\,p^{-1}\right)e^{-\beta y}+\gamma Ce^{-\gamma y}\ . \tag{60}$$

Next, in preparation for formulating a Wiener-Hopf equation, the one-sided Laplace transforms of the unknown stress $\sigma_{yx}\left(x>0,\,y=0\right)$ ahead of the crack tip, and the unknown crack-face displacement $u_{x}\left(x<0,\,y=0\right)$ are defined as follows

$$\Sigma^{+}\left(p\right)=\int_{0}^{\infty}\sigma_{yx}\left(x,y=0\right)e^{-px}dx\ , \tag{61a}$$

$$\sigma_{yx}\left(x,y=0\right)=\frac{1}{2\pi\mathrm{i}}\int_{Br}\Sigma^{+}\left(p\right)e^{px}dp\ , \tag{61b}$$

and

$$U^{-}\left(p\right)=\int_{-\infty}^{0}u_{x}\left(x,y=0\right)e^{-px}dx\ , \tag{62a}$$

$$u_{x}\left(x,y=0\right)=\frac{1}{2\pi\mathrm{i}}\int_{Br}U^{-}\left(p\right)e^{px}dp\ , \tag{62b}$$

where the Bromwich path is considered to lie inside the region of analyticity of each transformed function. In particular, we assume the following *finiteness conditions* at $x\to\pm\infty$: $\left|\sigma_{yx}\left(x,y=0\right)\right|<M\cdot\exp\left(-p_{\Sigma}x\right)$ for $x\to+\infty$ and $\left|u_{x}\left(x,y=0\right)\right|<N\cdot\exp\left(p_{U}x\right)$ for $x\to-\infty$, where $\left(M,N,p_{\Sigma},p_{U}\right)$ are positive constants. Consequently, the transformed function $\Sigma^{+}\left(p\right)$ is analytic and defined in the right half-plane $-p_{\Sigma}<\mathrm{Re}\left(p\right)$, while $U^{-}\left(p\right)$ is analytic and defined in the left half-plane $\mathrm{Re}\left(p\right)<p_{U}$.

Enforcing the boundary conditions (46) and (47) results in the following equations

$$\beta B+\gamma C=0\ , \tag{63}$$

$$A=0\ , \tag{64}$$

where the functions $B(p)$ and $D(p)$ are related through the Eqs. (40) and (41) as follows

$$B = 4(1-\nu)\ell^2 pD \ . \tag{65}$$

Consequently, Eqs. (45), (48), (57) and (60) lead to the following expressions

$$\Sigma^+(p) - Se^{Lp} = -pD\left[1 - 4p^2\ell^2(1-\nu)\left(1-\frac{\beta}{\gamma}\right)\right], \tag{66}$$

$$U^-(p) = -\frac{(1-\nu)\beta D}{\mu p}, \tag{67}$$

which provide the final functional (Wiener-Hopf) equation of the problem, connecting the two unknown functions $\Sigma^+(p)$ and $U^-(p)$

$$\Sigma^+(p) - Se^{Lp} = \frac{\mu p^2}{(1-\nu)\gamma} K(p) U^-(p) \ . \tag{68}$$

The kernel function $K(p)$ is given as

$$K(p) = 4(1-\nu)\ell^2 p^2 + \left[1 - 4(1-\nu)\ell^2 p^2\right]\frac{\gamma}{\beta} \ . \tag{69}$$

The problem has now been reduced to the determination of the unknown functions $\Sigma^+(p)$ and $U^-(p)$ from the single equation (68). At this point, we notice that the standard Wiener-Hopf technique needs a modification because the term e^{Lp} is unbounded as $|p| \to \infty$. This behavior leads to an unfortunate consequence of Liouville's theorem, which is indispensable in applying the Wiener-Hopf technique. More specifically, the entire function that emerges from the standard procedure (by applying Liouville's theorem and the principle of analytic continuation) is a polynomial of infinite order with unknown coefficients that cannot be evaluated from the given natural conditions of the problem. To circumvent this difficulty we follow here the analytic-function technique introduced by Georgiadis and Brock [48]. This technique utilizes simple contour integration along with a product kernel factorization.

To proceed further a product-factorization of the kernel $K(p)$ is required. First it is checked that $K(p)$ has no zeros in the complex plane. This was verified independently by using both the principle of the argument [56] and the symbolic computer program MATHEMATICA^{TM}. Next, we find that the asymptotic behavior of the kernel is $\lim_{|p|\to\infty} K(p) = 3-2\nu$. This leads us to introduce a modified kernel given as $N(p) = K(p)/(3-2\nu)$, which possesses the desired asymptotic property $\lim_{|p|\to\infty} N(p) = 1$. Indeed, this new form of the kernel facilitates its product splitting by the use of Cauchy's integral theorem (see e.g. [57,58]). The functional equation (68) takes now the form

$$\Sigma^{+}(p)(a+p)^{1/2} - Se^{Lp}(a+p)^{1/2} = \frac{\mu(3-2\nu)}{1-\nu}\cdot\frac{p^2 N(p)}{(a-p)^{1/2}}U^{-}(p)\ , \tag{70}$$

where the functions $\beta(p)$ and $\gamma(p)$ are written as products of two analytic and nonzero functions defined in the pertinent half-plane domains of the complex plane

$$\beta(p) = \beta^{+}(p)\cdot\beta^{-}(p) \equiv (\varepsilon+p)^{1/2}\cdot(\varepsilon-p)^{1/2}\ , \tag{71}$$

$$\gamma(p) = \gamma^{+}(p)\cdot\gamma^{-}(p) \equiv (a+p)^{1/2}\cdot(a-p)^{1/2}\ . \tag{72}$$

In addition, the modified kernel splits up as

$$N(p) = N^{+}(p)\cdot N^{-}(p)\ , \tag{73}$$

where

$$N^{+}(p) = \exp\left\{-\frac{1}{2\pi\mathrm{i}}\int_{C_l}\frac{\ln[N(\zeta)]}{\zeta-p}d\zeta\right\}\ , \tag{74a}$$

$$N^{-}(p) = \exp\left\{\frac{1}{2\pi\mathrm{i}}\int_{C_r}\frac{\ln[N(\zeta)]}{\zeta-p}d\zeta\right\}\ . \tag{74b}$$

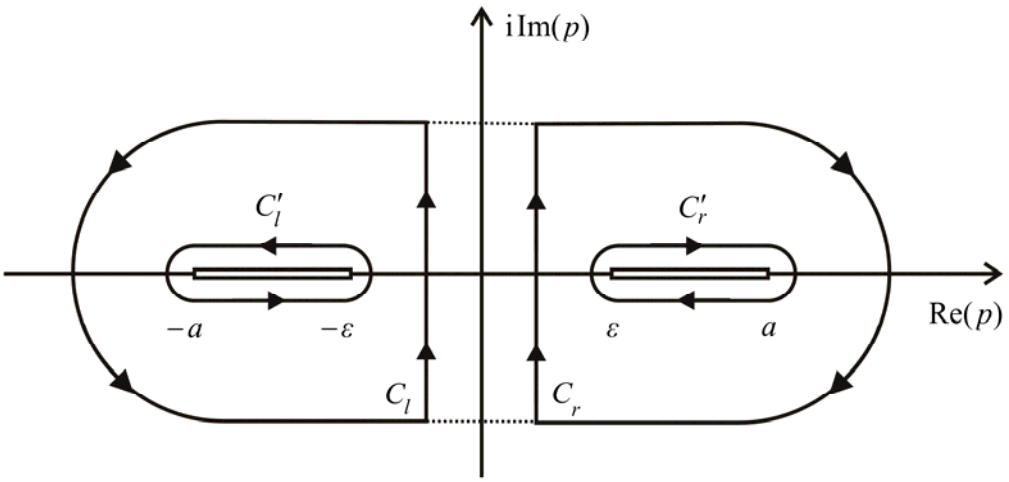

Figure 3. Contour integrations for the factorization of the kernel function $N(p)$.

The use of the Cauchy integral theorem is depicted in Figure 3. The functions $N^{+}(p)$ and $N^{-}(p)$ are analytic and nonzero in the half-planes $\mathrm{Re}(p) > -\varepsilon$ and $\mathrm{Re}(p) < \varepsilon$, respectively. The original integration paths C_l and C_r extend parallel to the imaginary axis in the complex ζ-plane. According to the Cauchy integral theorem and Jordan's lemma, we are allowed to use equivalent integration paths, i.e. the (C_l', C_r') contours around the branch cuts of $N(p)$ extending along $-a < \zeta < -\varepsilon$ and $\varepsilon < \zeta < a$. This eventually leads to the following forms of the sectionally analytic functions $N^{\pm}(p)$ (see Appendix A for details)

$$N^{\pm}(p) = \exp\left\{ \frac{1}{\pi} \int_0^a \tan^{-1}\left[\frac{\left(1-4(1-\nu)\ell^2\zeta^2\right)}{4(1-\nu)\ell^3} \cdot \frac{\left(1-\ell^2\zeta^2\right)^{1/2}}{\zeta^3} \right] \frac{d\zeta}{\zeta \pm p} \right\}, \tag{75}$$

with the properties $N^{+}(-p) = N^{-}(p)$ and $\lim_{|p|\to\infty} N^{\pm}(p) = 1$. It is noted that when p approaches the branch cuts in the ζ-plane from above or below, the integrals defining the functions $N^{+}(p)$ or $N^{-}(p)$ become singular. However, these integrals are not singular simultaneously. Thus, we may calculate these exceptional cases without resorting to principal values by employing

$N^{\pm}(p)=N(p)/N^{\mp}(p)$, where we choose in the denominator the $N^{\pm}(p)$ function that is not defined by a singular integral.

In view of the above, Eq. (70) can now be rewritten as

$$\frac{\Sigma^{+}(p)(a+p)^{1/2}}{N^{+}(p)}-\frac{Se^{Lp}(a+p)^{1/2}}{N^{+}(p)}=\frac{\mu(3-2\nu)}{1-\nu}\cdot\frac{p^{2}}{(a-p)^{1/2}}N^{-}(p)U^{-}(p)\ , \tag{76}$$

which holds in the strip $-\varepsilon<\mathrm{Re}(p)<\varepsilon$.

Next, in order to obtain the functions Σ^{+} and U^{-} from equation (76), it is convenient to change the variable from p to ω (the latter variable should not be confused with the rotation field in the original problem) and divide both sides of (76) by $2\pi\mathrm{i}(\omega-p)$, getting

$$\frac{\Sigma^{+}(\omega)(a+\omega)^{1/2}}{2\pi\mathrm{i}(\omega-p)N^{+}(\omega)}-\frac{Se^{L\omega}(a+\omega)^{1/2}}{2\pi\mathrm{i}(\omega-p)N^{+}(\omega)}=\frac{\mu(3-2\nu)}{1-\nu}\cdot\frac{\omega^{2}N^{-}(\omega)U^{-}(\omega)}{2\pi\mathrm{i}(\omega-p)(a-\omega)^{1/2}}\ . \tag{77}$$

By taking the point p to lie in the right half-plane $\mathrm{Re}(\omega)>0$, Eq.(77) can be integrated over the imaginary axis $\mathrm{i}\,\mathrm{Im}(\omega)$ to yield the result

$$\frac{1}{2\pi\mathrm{i}}\int_{-\mathrm{i}\infty}^{+\mathrm{i}\infty}\frac{\Sigma^{+}(\omega)(a+\omega)^{1/2}}{N^{+}(\omega)(\omega-p)}d\omega-\frac{S}{2\pi\mathrm{i}}\int_{-\mathrm{i}\infty}^{+\mathrm{i}\infty}\frac{e^{L\omega}(a+\omega)^{1/2}}{N^{+}(\omega)(\omega-p)}d\omega=$$

$$=\frac{\mu(3-2\nu)}{2\pi\mathrm{i}(1-\nu)}\int_{-\mathrm{i}\infty}^{+\mathrm{i}\infty}\frac{\omega^{2}N^{-}(\omega)U^{-}(\omega)}{(a-\omega)^{1/2}(\omega-p)}\,d\omega\ . \tag{78}$$

We now intend to deform the integration path $(-\mathrm{i}\infty,+\mathrm{i}\infty)$ by using large semi-circles in the left and right half-planes, in order to exploit Cauchy's theorem and Cauchy's integral formula. Since integration will include large semi-circular paths at infinity, it is first necessary to examine the asymptotic behavior of the functions $\Sigma^{+}(\omega)$ and $U^{-}(\omega)$, entering the integrals in (78). This behavior is not clear in advance. Thus, we examine several possibilities, in light also of previous asymptotic results obtained for the remote-loading case [16].

First, we examine the following possible behavior for the stress and crack-face displacement along the crack faces, which coincides with the corresponding classical case

$$\sigma_{yx}(x, y=0) = O\left(x^{-1/2}\right) \quad \text{as} \quad x \to +0 \ , \tag{79}$$

$$u_x(x, y=0) = O\left(x^{1/2}\right) \quad \text{as} \quad x \to -0 \ . \tag{80}$$

This asymptotic behavior has been obtained by Huang et al. [16,17] for the problem of a plane-strain crack subjected to remotely applied shear loading (mode-II case), within the context of couple-stress theory. Such a behavior was also corroborated by the uniqueness theorem for crack problems of couple-stress elasticity which imposes the requirement of boundedness for both crack-tip displacement and rotation (Grentzelou and Georgiadis [25]).

Further, we consider at this point the transformation formula $x^{\kappa} \overset{LT}{\leftrightarrow} \Gamma(\kappa+1) \cdot p^{-\kappa-1}$ (with $\kappa \neq -1, -2, -3, \ldots$), where $\Gamma(\ )$ is the Gamma function with $\kappa > -1$ [55,57]. The symbol $\overset{LT}{\leftrightarrow}$ means that the quantities on either side of the arrow are connected through the one-sided Laplace-transform. In light of the above, and employing theorems of the Abel-Tauber type (see e.g. [57]), we obtain the following asymptotic behavior in the transform domain

$$\Sigma^{+}(\omega) = O\left(\omega^{-1/2}\right) \quad \text{as} \quad |\omega| \to \infty \quad \text{with} \quad \mathrm{Re}(\omega) > 0 \ , \tag{81}$$

$$U^{-}(\omega) = O\left(\omega^{-3/2}\right) \quad \text{as} \quad |\omega| \to \infty \quad \text{with} \quad \mathrm{Re}(\omega) < 0 \ . \tag{82}$$

Now, for the first integral in (78) we choose to close the integration path with a large semi-circle at infinity in the right half-plane $(\mathrm{Re}(\omega) > 0)$, with a radius that tends to infinity, and then use Cauchy's integral formula. For the third integral, we close the integration path with a large semi-circle at infinity in the left half-plane $(\mathrm{Re}(\omega) < 0)$, where the integrand is an analytic function. Then, bearing in mind that p belongs to the right half plane, Eq. (78) becomes

$$-\frac{\Sigma^{+}(p)(a+p)^{1/2}}{N^{+}(p)} - D - \frac{S}{2\pi \mathrm{i}} \int_{-\mathrm{i}\infty}^{+\mathrm{i}\infty} \frac{e^{L\omega}(a+p)^{1/2}}{N^{+}(\omega)(\omega - p)} d\omega = E \ , \tag{83}$$

which, equivalently, gives the transformed solution for the shear stress ahead of the crack-tip as

$$\Sigma^{+}\left(p\right)=-\left(a+p\right)^{-1/2}N^{+}\left(p\right)\cdot\frac{S}{2\pi\mathrm{i}}\int_{-\mathrm{i}\infty}^{+\mathrm{i}\infty}\frac{e^{L\omega}\left(a+\omega\right)^{1/2}}{N^{+}\left(\omega\right)\left(\omega-p\right)}d\omega-\Delta\cdot\left(a+p\right)^{-1/2}N^{+}\left(p\right)\,, \tag{84}$$

where $\Delta=D+E$ is the algebraic sum of the two constants (D,E) that emerge from the integration, along the corresponding semi-circular paths with radius R, of the first and third integral in (78). The latter integrals are of the form $O\left(R^{0}\right)$ as $R\to\infty$.

Next, we consider another possibility of near-tip behavior (this is the response predicted by the dipolar gradient theory [30])

$$\sigma_{yx}\left(x,y=0\right)=O\left(x^{-3/2}\right)\quad\text{as}\quad x\to+0\,, \tag{85}$$

$$u_{x}\left(x,y=0\right)=O\left(x^{3/2}\right)\quad\text{as}\quad x\to-0\,. \tag{86}$$

Moreover, by using certain results of the theory of generalized functions concerning transforms of singular distributions [59,60], we obtain the following asymptotic behavior in the transform domain

$$\Sigma^{+}\left(\omega\right)=O\left(\omega^{1/2}\right)\quad\text{as}\quad|\omega|\to\infty\quad\text{with}\quad\mathrm{Re}\left(\omega\right)>0\,, \tag{87}$$

$$U^{-}\left(\omega\right)=O\left(\omega^{-5/2}\right)\quad\text{as}\quad|\omega|\to\infty\quad\text{with}\quad\mathrm{Re}\left(\omega\right)<0\,. \tag{88}$$

In this case, due to the asymptotic behavior of the integrand of the first integral in Eq. (78), we get an infinite value from the contribution of the semi-circular path of integration as $|\omega|\to\infty$. This result is inadmissible upon considering an inversion in the physical plane. Therefore, the possibility of a near-tip behavior given by (85) and (86) should be discarded. Finally, any other case like, e.g., $\sigma_{yx}=O\left(x^{-1}\right)$ or $\sigma_{yx}=O\left(x^{-2}\right)$, as $x\to+0$, is precluded since even analytic continuation fails to define one-sided Laplace transforms of the associated singular distributions [59].

Returning now back to Eq. (83), we proceed to calculate the integral by deforming the integration path in the left half-plane (see Fig. B.1 in Appendix B) where the integrand is non-analytic, exploiting in this way the existence of branch cuts for the functions $N^{+}\left(\omega\right)$ and $\left(a+\omega\right)^{1/2}$. Further, recalling that $\lim_{|\omega|\to\infty}N^{+}\left(\omega\right)=1$ and also that $N^{+}\left(\omega\right)=N\left(\omega\right)/N^{-}\left(\omega\right)$ (cf. Eq. (73)), the integral in (83) is written by Cauchy's theorem as (for the details of the derivation see Appendix B)

$$\frac{1}{2\pi \mathrm{i}}\int_{-\mathrm{i}\infty}^{+\mathrm{i}\infty}\frac{e^{L\omega}\left(a+\omega\right)^{1/2}}{N^{+}\left(\omega\right)\left(\omega-p\right)}d\omega=\frac{1}{\pi}G\left(p\right)\ , \tag{89}$$

where

$$G\left(p\right)=\int_{0}^{a}\frac{f\left(\omega\right)}{\omega+p}d\omega+\int_{a}^{\infty}\frac{h\left(\omega\right)}{\omega+p}d\omega\ \ , \tag{90}$$

and the functions $f\left(\omega\right),\ h\left(\omega\right)$ are defined as

$$f\left(\omega\right)=\frac{N^{+}\left(\omega\right)\left[\operatorname{Im}N\left(\omega\right)\right]\left|a-\omega\right|^{1/2}\ e^{-L\omega}}{\left[\operatorname{Re}N\left(\omega\right)\right]^{2}+\left[\operatorname{Im}N\left(\omega\right)\right]^{2}}\ ,\qquad h\left(\omega\right)=\frac{e^{-L\omega}\left|a-\omega\right|^{1/2}}{N^{-}\left(\omega\right)}\ . \tag{91a,b}$$

The real and imaginary parts above are given by the expressions

$$\operatorname{Re}N\left(\omega\right)=\frac{4\left(1-\nu\right)\ell^{2}\omega^{2}}{3-2\nu}\ ,\quad \operatorname{Im}N\left(\omega\right)=\frac{\left[1-4\left(1-\nu\right)\ell^{2}\omega^{2}\right]\left(a^{2}-\omega^{2}\right)^{1/2}}{\left(3-2\nu\right)\omega}\quad \text{for}\quad 0<\omega\le a\ . \tag{92a,b}$$

Our task now is to evaluate the constant Δ. This is accomplished by examining the asymptotic behavior of the solution in (84) as $p\to+0$, i.e. as $x\to+\infty$ in the physical plane. First, the limit of the function $G\left(p\right)$ will be determined. To this end, use is made of the following series expansion

$$\left(1+\frac{p}{\omega}\right)^{-1}=1-\frac{p}{\omega}+\left(\frac{p}{\omega}\right)^{2}-\ldots\qquad \text{for}\ \ \left|\frac{p}{\omega}\right|<1\ . \tag{93}$$

Thus, we obtain

$$\lim_{p\to+0}G\left(p\right)=\left[\int_{0}^{a}\frac{f\left(\omega\right)}{\omega}d\omega+\int_{a}^{\infty}\frac{h\left(\omega\right)}{\omega}d\omega\right]-p\left[\int_{0}^{a}\frac{f\left(\omega\right)}{\omega^{2}}d\omega+\int_{a}^{\infty}\frac{h\left(\omega\right)}{\omega^{2}}d\omega\right]+O\left(p^{2}\right)\ . \tag{94}$$

Next, the limits of $N^{\pm}(p)$ as $p \to 0$ will be established. This can be done by performing a product factorization of the limit value $\lim_{|p|\to 0} N(p)$ by *inspection*. Indeed, one may obtain first from (69) and the definition of $N(p)$ the limit $\lim_{|p|\to 0} N(p) = a(3-2\nu)^{-1}\left(\varepsilon^2 - p^2\right)^{-1/2}$ and then

$$\lim_{|p|\to 0} N^{\pm}(p) = a^{1/2}(3-2\nu)^{-1/2}(\pm p)^{-1/2} \ . \tag{95}$$

Further, a combination of (84), (94) and (95) provides the limit

$$\lim_{|p|\to 0} \Sigma^{+}(p) = -\frac{S}{\pi(3-2\nu)^{1/2}} \cdot \left\{ \left[\int_0^a \frac{f(\omega)}{\omega} d\omega + \int_a^{\infty} \frac{h(\omega)}{\omega} d\omega + \frac{\pi}{S}\Delta \right] p^{-1/2} - \right.$$
$$\left. - \left[\text{F.P.} \int_0^a \frac{f(\omega)}{\omega^2} d\omega + \int_a^{\infty} \frac{h(\omega)}{\omega^2} d\omega \right] p^{1/2} + O\left(p^{3/2}\right) \right\} , \tag{96}$$

where the symbol $\text{F.P.}\int$ indicates finite-part integration [61,62].

The argument now leading to the evaluation of the constant Δ has as follows. Since a behavior of the shear stress at $x \to +\infty$ of the form $\sigma_{yx} \sim x^{-1/2}$ is precluded due to the existence of the concentrated load at $(x = -L,\ y = 0)$, the only possibility left from (96) is the vanishing of the term inside the first bracket, i.e. the following relation

$$\Delta = -\frac{S}{\pi}\left[\int_0^a \frac{f(\omega)}{\omega} d\omega + \int_a^{\infty} \frac{h(\omega)}{\omega} d\omega \right] \equiv -\frac{S}{\pi} G_0 \ . \tag{97}$$

The above argument is supported also by the form of the solution as $x \to +\infty$ in the respective problem of classical elasticity, where $\sigma_{yx} \sim x^{-3/2}$ [63]. Indeed, Eqs. (96) and (97) lead to a similar $\sim x^{-3/2}$ behavior for the shear stress as $x \to +\infty$. Moreover, it should be noted that since $f(\omega)/\omega^2 = O\left(\omega^{-3/2}\right)$ as $\omega \to +0$, the first integral in the second bracket of (96) should be understood in the finite-part sense [61,62].

Finally, using (84) in conjunction with (89) and (97), we obtain the following expression for the transformed shear stress

$$\Sigma^{+}(p)=-\frac{S}{\pi}(a+p)^{-1/2}N^{+}(p)\cdot\left[G(p)-G_0\right]\ ,\quad \mathrm{Re}(p)>0\ . \tag{98}$$

Also, according to Eqs. (70) and (98), and by using analytic continuation arguments, one may write the following expression for the transformed displacement (valid for all p in the pertinent half-plane of convergence)

$$U^{-}(p)=-\frac{S(1-\nu)}{\mu(3-2\nu)}\left\{\frac{1}{\pi}\frac{(a-p)^{1/2}}{p^2N^{-}(p)}\left[G(p)-G_0\right]+\frac{e^{Lp}\left(a^2-p^2\right)^{1/2}}{p^2N(p)}\right\}\ ,\qquad \mathrm{Re}(p)<0\ . \tag{99}$$

5. BASIC ASYMPTOTIC RESULTS

5.1. Evaluation of the Stress Intensity Factor

The Abel-Tauber theorem, is utilized to obtain the singular part of stress, $\lim_{x\to+0}\sigma_{yx}(x,0)$, from the large-$p$ approximation ($|p|\to\infty$) of Eq. (98). Indeed, with the approximation $\omega+|p|\approx|p|$, the variable p can be extracted from the integrand of the integral $G(p)$. Notice also that the function $h(\omega)$ defined in (91b) rapidly decays as $\omega\to\infty$. Therefore, the integral $G(p)$ can be expressed asymptotically as

$$\lim_{|p|\to\infty}G(p)=\lim_{|p|\to\infty}\left[\int_0^a\frac{f(\omega)}{\omega+p}d\omega+\int_a^\infty\frac{h(\omega)}{\omega+p}d\omega\right]=\frac{1}{p}\cdot G_1\ , \tag{100}$$

where $G_1=\int_0^a f(\omega)d\omega+\int_a^\infty h(\omega)d\omega$.

Consequently, from (98) and (100), and taking into account that $\lim_{|p|\to\infty}N^{+}(p)=1$, one readily finds that

$$\lim_{|p|\to\infty} \Sigma^{+}(p) = \frac{S}{\pi} G_0 \, p^{-1/2} \ . \tag{101}$$

Also, using similar arguments, the limit of the solution (99) at infinity is

$$\lim_{|p|\to\infty} U^{-}(p) = \frac{S(1-\nu)G_0}{\pi\mu(3-2\nu)} p^{-3/2} \ . \tag{102}$$

Now, from the Abel-Tauber theorem, we obtain the following near-tip field

$$\lim_{x\to+0} \sigma_{yx}(x, y=0) = \frac{SG_0}{\pi^{3/2}} x^{-1/2} \ , \tag{103}$$

$$\lim_{x\to-0} u_x(x, y=0) = \frac{2S(1-\nu)G_0}{\mu\pi^{3/2}(3-2\nu)} (-x)^{1/2} \ . \tag{104}$$

Then, according to Eq. (103) and the definition $K_{II} = \lim_{x\to+0} (2\pi x)^{1/2} \sigma_{yx}(x, y=0)$, the ratio of the stress intensity factor (SIF) in couple-stress elasticity over the SIF provided by the classical elasticity becomes

$$\frac{K_{II}}{K_{II}^{clas.}} = G_0 \left(\frac{L}{\pi} \right)^{1/2} \ . \tag{105}$$

where $K_{II}^{clas.} = S(2/\pi L)^{1/2}$ is the SIF provided by classical elasticity (see e.g. [63]). The numerical computation of the integral G_0 (which was defined in (97)) entering the above expression was achieved by the use of the computer program MATHEMATICA™ (version 7).

Figure 4 depicts the variation of the ratio $K_{II}/K_{II}^{clas.}$ with ℓ/L for three different values of the Poisson's ratio. It can be shown that the ratio in (105) has the asymptote $(3-2\nu)^{1/2}$ as $\ell/L \to 0$. It is worth noting, that the same result was previously obtained by Huang et al. [17] for a semi-infinite crack under remote shear loading, and by Gourgiotis and Georgiadis [41] in the case of a mode II central finite-length crack when $\ell/a \to 0$ ($2a$ being the length of the crack). On the other hand, when $\ell/L = 0$ (no couple-stress effects), the above ratio should evidently become $K_{II}/K_{II}^{clas.} = 1$.

However, the ratio plotted in Fig. 4 exhibits a finite jump *discontinuity* at the limit $\ell/L=0$; the ratio at the tip of the crack rises abruptly as ℓ/L departs from zero. The same discontinuity was observed by Sternberg and Muki [39] and by Gourgiotis and Georgiadis [41,42], who attributed this behavior to the severe boundary layer effects of couple-stress elasticity in singular stress-concentration problems. We also observe that unlike the case of the finite-length traction-free crack [41,42], the ratio does not decrease monotonically with increasing values of ℓ/L. Indeed, the ratio $K_{II}/K_{II}^{clas.}$ exhibits a bounded maximum when the material microstructure becomes comparable with geometric length L. In particular, it is observed that for $\ell/L=0.2$ and Poisson's ratio $\nu=0.25$, there is a maximum 72% increase in K_{II} when couple-stress effects are taken into account, while for $\nu=0$ the increase is 92%. Finally, it can be shown that the ratio tends to unity as $\ell/L\to\infty$.

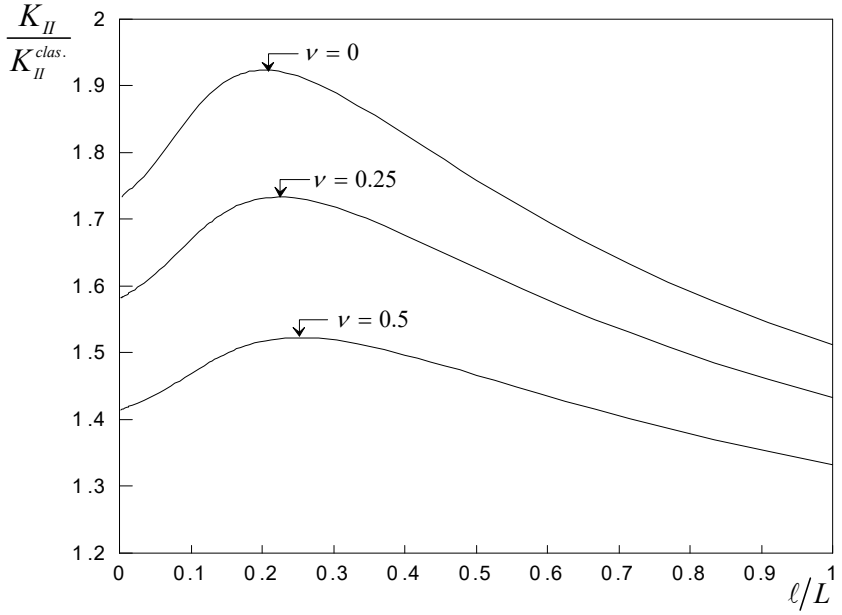

Figure 4. Variation of the ratio of stress intensity factors in couple-stress elasticity and in classical elasticity with ℓ/L.

5.2. Evaluation of the J-Integral

In this Section, we evaluate the J-integral (energy release rate) of Fracture Mechanics and examine its dependence upon the ratio of lengths ℓ/L and the Poisson's ratio ν. The J-integral in

couple-stress elasticity was first established by Atkinson and Leppington [64] (see also [19] and [40]) and is written as

$$J=\int_{\Gamma}\left[Wn_x-T_q^{(n)}\frac{\partial u_q}{\partial x}-M_q^{(n)}\frac{\partial \omega_q}{\partial x}\right]d\Gamma=\int_{\Gamma}\left[Wn_x-P_q^{(n)}\frac{\partial u_q}{\partial x}-R_q^{(n)}\frac{\partial \omega_q}{\partial x}\right]d\Gamma$$
$$=\int_{\Gamma}\left(Wdy-\left[P_q^{(n)}\frac{\partial u_q}{\partial x}+R_q^{(n)}\frac{\partial \omega_q}{\partial x}\right]d\Gamma\right), \tag{106}$$

where Γ is a piecewise smooth simple 2D contour surrounding the crack-tip, W is the strain-energy density, $(T_q^{(n)},M_q^{(n)})$ are the tractions defined in (3) and (4), and $(P_q^{(n)},R_q^{(n)})$ are the reduced force-traction and tangential couple-traction defined in (18) and (19). Moreover, we note that in the expression for the J-integral in (106), the edge forces are not included since the latter are zero in plane strain (see also Section 3). However, in the context of dipolar gradient elasticity these edge forces contribute to the energy release rate, and, therefore, should be taken into account [54]. A more general analysis of the energy release rate in the context of finite-strain polar elasticity was provided by Maugin [65].

For the evaluation of the J-integral, we consider the rectangular-shaped contour Γ (surrounding the crack-tip) with vanishing 'height' along the y- direction and with $\varepsilon\to+0$ (see Fig. 5). Such a contour was first introduced by Freund [66] in examining the energy flux into the tip of a rapidly extending crack and it was proved particularly convenient in computing energy quantities in the vicinity of crack tips (see e.g. [21,67]). In fact, this type of contour permits using solely the *asymptotic* near-tip stress and displacement fields. It is noted that upon this choice of contour, the integral $\int_{\Gamma}W\,dy$ in (106) becomes zero if we allow the 'height' of the rectangle to vanish. In this way, the expression for the J-integral becomes

$$J=-2\lim_{\varepsilon\to+0}\left\{\int_{-\varepsilon}^{\varepsilon}\left(P_q^{(n)}\frac{\partial u_q}{\partial x}+R_q^{(n)}\frac{\partial \omega_q}{\partial x}\right)dx\right\}. \tag{107}$$

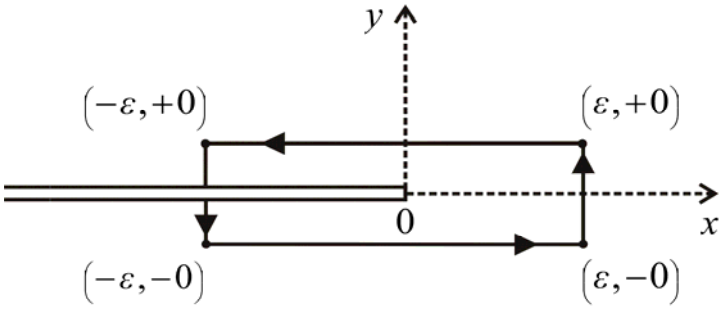

Figure 5. Rectangular-shaped contour surrounding the crack-tip.

Further, we note that due to the antisymmetry conditions that prevail in the mode II case, the normal stress σ_{yy} and the couple-stress m_{yz} are zero along the whole crack line $(y=0)$, whereas the crack-faces are defined by $\mathbf{n}=(0,\pm 1)$. Then, the J-integral in (107) assumes the form

$$J=-2\lim_{\varepsilon\to+0}\left\{\int_{-\varepsilon}^{\varepsilon}\left[\sigma_{yy}\left(x,y=0^{+}\right)\cdot\frac{\partial u_y\left(x,y=0^{+}\right)}{\partial x}+\sigma_{yx}\left(x,y=0^{+}\right)\cdot\frac{\partial u_x\left(x,y=0^{+}\right)}{\partial x}\right.\right.$$
$$\left.\left.+m_{yz}\left(x,y=0^{+}\right)\cdot\frac{\partial\omega\left(x,y=0^{+}\right)}{\partial x}\right]dx\right\}$$
$$=-2\lim_{\varepsilon\to+0}\left\{\int_{-\varepsilon}^{\varepsilon}\sigma_{yx}\left(x,y=0^{+}\right)\cdot\frac{\partial u_x\left(x,y=0^{+}\right)}{\partial x}\,dx\right\}. \qquad (108)$$

Now, by using the asymptotic solution (103) and (104), we finally obtain

$$J=\lim_{\varepsilon\to 0}\left\{\frac{2S^2(1-\nu)G_0^2}{\mu\pi^3(3-2\nu)}\cdot\int_{-\varepsilon}^{\varepsilon}(x_+)^{-1/2}(x_-)^{-1/2}\,dx\right\}, \qquad (109)$$

where for any real λ with the exception of $\lambda=-1,-2,-3,\ldots$, the following definitions of the distributions (of the bisection type) x_+^{λ} and x_-^{λ} are employed [59]

$$x_+^\lambda = \begin{cases} |x|^\lambda, & \text{for } x>0 \\ \\ 0, & \text{for } x<0 \end{cases} \quad \text{and} \quad x_-^\lambda = \begin{cases} 0, & \text{for } x>0 \\ \\ |x|^\lambda, & \text{for } x<0 \end{cases} . \tag{110}$$

Moreover, the product of distributions inside the integral in (109) is obtained through the use of Fisher's theorem [68], i.e. the operational relation $(x_-)^\lambda (x_+)^{-1-\lambda} = -\pi\,\delta(x)\left[2\sin(\pi\lambda)\right]^{-1}$ with $\lambda \neq -1,-2,-3,...$ and $\delta(x)$ being the Dirac delta distribution. Then, in view of the fundamental property of Dirac delta distribution that $\int_{-\varepsilon}^{\varepsilon} \delta(x)\,dx = 1$, Eq. (109) provides the result

$$J = \frac{S^2(1-\nu)G_0^2}{\mu\pi^2(3-2\nu)} . \tag{111}$$

Based on the above analysis, we were able to evaluate the J-integral. Our results are shown in the graph of Figure 6 that depicts the dependence of the ratio $J/J^{clas.}$ upon the ratio of lengths ℓ/L for three different values of the Poisson's ratio of the material. The quantity $J^{clas.} = S^2(1-\nu)/(\mu\pi L)$ is the respective integral in classical elasticity (see e.g. Freund [69]).

The calculations show that as $\ell/L \to 0$, the J-integral in couple-stress elasticity tends continuously to its classical counterpart. Moreover, as ℓ/L increases form zero, the ratio $J/J^{clas.}$ increases exhibiting a bounded maximum in the range $0.2 \le \ell/L \le 0.25$ (that depends on the Poisson's ratio). This finding is in contrast with previous results concerning the case of a finite-length traction-free crack [41,42], and the case of a semi-infinite crack with distributed normal loading along the crack faces [40]. Indeed, in the latter cases, the ratio $J/J^{clas.}$ decreased monotonically with increasing values of the material length ℓ to the pertinent geometrical length. This change in the behavior of the J-integral is brought out more clearly in the next section, where we examine the case of a semi-infinite crack with distributed (exponentially decaying) shear loading along the crack faces (see also Fig. 8). Finally, it is worth noting that for $\ell/L \ge 0.55$ the ratio becomes less than unity and decreases monotonically to the limit $1/(3-2\nu)$ as $\ell/L \to \infty$.

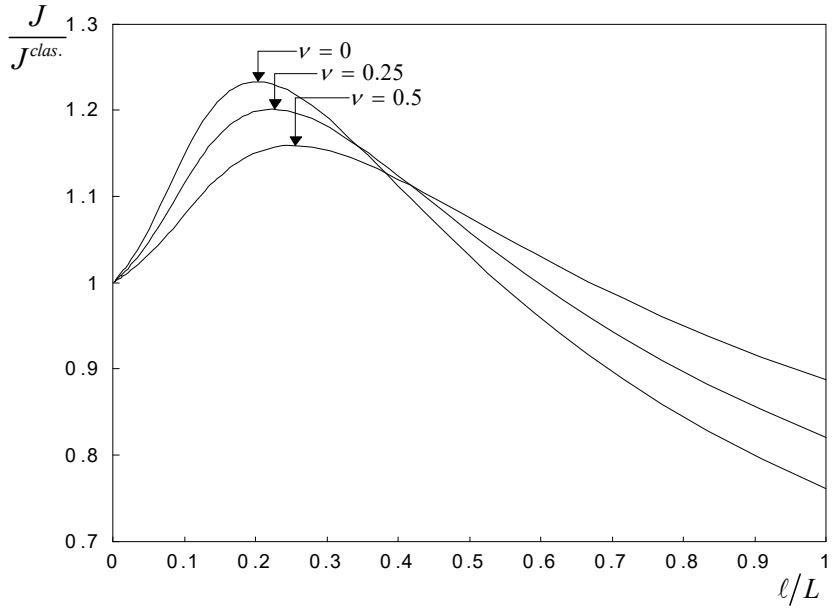

Figure 6. Variation of the ratio of the J -integrals in couple-stress elasticity and in classical elasticity with ℓ/L .

6. DISTRIBUTED SHEAR LOADING ALONG THE CRACK FACES

For the purpose of comparison with the problem analyzed before and for the purpose of completeness of the present study, the case of a semi-infinite crack with a distributed shear loading along the crack faces (see Fig. 7) is examined in this Section. The case of a semi-infinite crack with a distributed *normal* loading was treated by Atkinson and Leppington [40]. Regarding the variation of the distributed loading, we follow here their idea to consider tractions that are exponentially decaying from the crack tip. Instead, if uniform crack-face tractions were considered, an unbounded behavior of the solution would occur because a semi-infinite crack is involved in a body of infinite extent.

Since the analysis of the problem is analogous to that employed in the previous Sections, we omit details and cite directly the results obtained. The boundary conditions (46)-(48) still apply, but (45) is replaced by

$$\sigma_{yx}\left(y=0\right)=-\tau_0\, e^{x/\xi} \qquad \text{for} \quad -\infty < x < 0 \ , \tag{112}$$

where τ_0 and ξ are positive constants having pertinent dimensions.

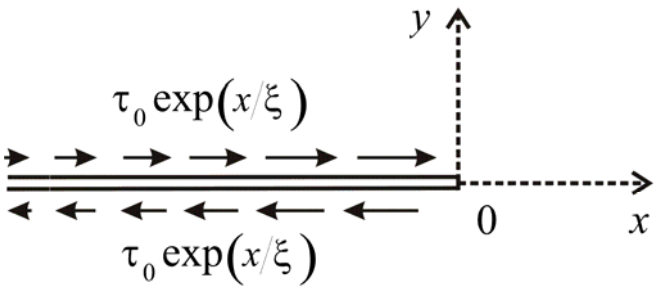

Figure 7. Semi-infinite crack with exponentially decaying shear loading along the crack faces.

The Wiener-Hopf equation in this case takes the following form

$$\frac{\Sigma^+(p)(a+p)^{1/2}}{N^+(p)}-\frac{\tau_0\xi(a+p)^{1/2}}{(1-\xi p)N^+(p)}=\frac{\mu(3-2\nu)}{1-\nu}\cdot\frac{p^2}{(a-p)^{1/2}}N^-(p)U^-(p)\ , \tag{113}$$

where the functions $\Sigma^+(p)$ and $U^-(p)$ are analytic in the pertinent half-planes, and $N^{\pm}(p)$ are defined in (75).

The sum-splitting of the second term in the LHS of (113) required to complete the decoupling process can now be obtained by inspection as

$$M(p)\equiv\frac{\tau_0\xi(a+p)^{1/2}}{(1-\xi p)N^+(p)}=M^+(p)+M^-(p)\ , \tag{114}$$

where

$$M^+(p)=\frac{\tau_0\xi}{(1-\xi p)}\left[\frac{(a+p)^{1/2}}{N^+(p)}-\frac{\left[a+(1/\xi)\right]^{1/2}}{N^+(1/\xi)}\right], \tag{115a}$$

$$M^-(p)=\frac{\tau_0\xi}{(1-\xi p)}\frac{\left[a+(1/\xi)\right]^{1/2}}{N^+(1/\xi)}\ , \tag{115b}$$

and $M^+(p)$ is an analytic function in the same right half-plane where $N^+(p)$ is defined, while $M^-(p)$ is an analytic function in the left half-plane where $\mathrm{Re}(p) < 1/\xi$. Equations (113) and (114), when combined, allow the final re-arrangement of the Wiener-Hopf equation

$$\frac{(a+p)^{1/2}\,\Sigma^+(p)}{N^+(p)} - M^+(p) = \frac{\mu(3-2\nu)}{1-\nu}\cdot\frac{p^2\,N^-(p)}{(a-p)^{1/2}}\,U^-(p) + M^-(p) \equiv E(p)\ . \tag{116}$$

The above functional equation defines the function $E(p)$ only in the strip $-\varepsilon < \mathrm{Re}(p) < \varepsilon$. Now, taking into account that $\Sigma^+ \sim p^{-1/2}$ and $U^- \sim p^{-3/2}$ as $|p| \to \infty$ (see also Eqs. (81)-(82)), we conclude that the first member of (116) is a bounded nonzero analytic function for $\mathrm{Re}(p) > -\varepsilon$, whereas the second member is a bounded nonzero analytic function for $\mathrm{Re}(p) < 0$. Then, in view of the theorem of analytic continuation, the two members define one and the same analytic function $E(p)$ over the entire complex p-plane [57,58]. Moreover, the extended Liouville's theorem leads to the conclusion that $E(p) = E_0$, where E_0 is a constant.

The transformed shear stress is given by (116) as

$$\Sigma^+(p) = \left[E_0 + M^+(p)\right] N^+(p)(a+p)^{-1/2}\ . \tag{117}$$

The constant E_0 will now be determined from conditions at remote regions in the physical plane. First, we observe that the exponentially decaying tractions in (112) can be replaced by a statically equivalent concentrated load of intensity: $\int_{-\infty}^{0} \sigma_{yx}\,dx = -\tau_0\xi$. Thus, according to Saint-Venant's principle (see e.g. [70]) and in view of the solution of the concentrated load problem treated in Section 4, we anticipate that the shear stress will behave as $\sim x^{-3/2}$ for $x \to +\infty$. This, in turn, implies the following asymptotic behavior in the transformed domain: $\Sigma^+(p) = O\left(p^{1/2}\right)$ as $p \to +0$. Further, taking into account (95) and (115a), we obtain the limit

$$\lim_{|p|\to 0} \Sigma^+(p) = (3-2\nu)^{-1/2}\left[E_0 - \frac{\tau_0\xi\left[a+(1/\xi)\right]^{1/2}}{N^+(1/\xi)}\right] p^{-1/2} + O\left(p^{1/2}\right)\ . \tag{118}$$

In view of the above, the only possibility left from (118) is the vanishing of the term inside the bracket, i.e.

$$E_0 = \frac{\tau_0 \xi \left[a + (1/\xi) \right]^{1/2}}{N^+ (1/\xi)} \ . \tag{119}$$

The final transformed expressions (valid for all p in the pertinent half-plane of convergence) for the stress ahead of the tip and the crack-face displacement then become

$$\Sigma^+ (p) = \left[\frac{\tau_0 \xi \left[a + (1/\xi) \right]^{1/2}}{N^+ (1/\xi)} + M^+ (p) \right] N^+ (p) (a+p)^{-1/2} \ , \quad \mathrm{Re}(p) > 0 \ , \tag{120}$$

$$U^- (p) = \frac{(1-\nu)}{\mu (3-2\nu)} \left[\frac{\tau_0 \xi \left[a + (1/\xi) \right]^{1/2}}{N^+ (1/\xi)} - M^- (p) \right] \frac{(a-p)^{1/2}}{p^2 N^- (p)} \ , \quad \mathrm{Re}(p) < 0 \ . \tag{121}$$

The limits of the latter expressions for $|p| \to \infty$ are found to be

$$\lim_{|p| \to \infty} \Sigma^+ (p) = \frac{\tau_0 \xi \left[a + (1/\xi) \right]^{1/2}}{N^+ (1/\xi)} p^{-1/2} , \tag{122}$$

$$\lim_{|p| \to \infty} U^- (p) = \frac{\tau_0 (1-\nu)}{\mu (3-2\nu)} \frac{\xi \left[a + (1/\xi) \right]^{1/2}}{N^+ (1/\xi)} p^{-3/2} \ , \tag{123}$$

which, accordingly, provide the following near-tip field

$$\lim_{x \to +0} \sigma_{yx} (x, y=0) = \frac{\tau_0 \xi \left[a + (1/\xi) \right]^{1/2}}{\pi^{1/2} N^+ (1/\xi)} x^{-1/2} \ . \tag{124}$$

$$\lim_{x \to -0} u_x (x, y=0) = \frac{2\tau_0 (1-\nu)}{\mu \pi^{1/2} (3-2\nu)} \frac{\xi \left[a + (1/\xi) \right]^{1/2}}{N^+ (1/\xi)} (-x)^{1/2} \ . \tag{125}$$

Moreover, following the same procedure as in Section 5, the stress intensity factor and the energy release rate in couple-stress elasticity are written as

$$K_{II}=\frac{2^{1/2}\tau_0\,\xi\left[a+(1/\xi)\right]^{1/2}}{N^{+}(1/\xi)}\ , \tag{126}$$

$$J=\frac{\tau_0^2\,\xi^2(1-\nu)}{\mu(3-2\nu)}\cdot\frac{\left[a+(1/\xi)\right]}{\left[N^{+}(1/\xi)\right]^2}\ . \tag{127}$$

We proceed now to the discussion of the numerical results obtained. The quantities of primary physical interest in this problem are the stress intensity factor and the energy release rate. Figure 8 depicts the variation of the ratio $K_{II}/K_{II}^{clas.}$ with ℓ/ξ for three different values of the Poisson's ratio. The stress intensity factor for the respective problem in classical elasticity is $K_{II}^{clas.}=\tau_0(2\xi)^{1/2}$. As in the concentrated load case (Section 4), the ratio plotted in Fig. 8 exhibits a finite jump discontinuity at the limit $\ell/\xi=0$; the ratio at the tip of the crack rises abruptly as ℓ/ξ departs from zero. In particular, it can be shown that $K_{II}/K_{II}^{clas.}\to(3-2\nu)^{1/2}$ as $\ell/\xi\to 0$. Moreover, for $\ell/\xi\to\infty$, the ratio tends to unity. However, a fundamental difference between the two cases is that the ratio here decreases monotonically with increasing values of ℓ/ξ. The same behavior was observed in the case of a mode II finite-length crack in couple-stress elasticity [41].

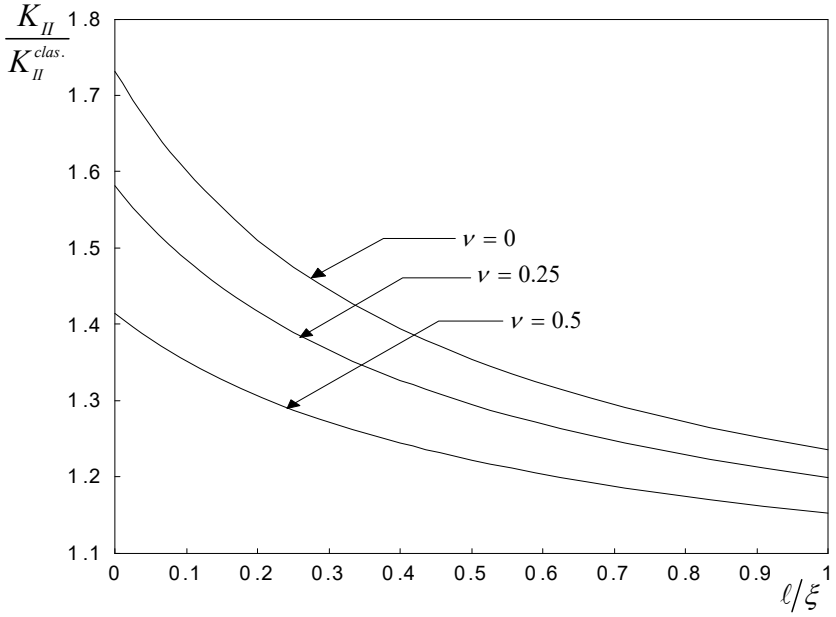

Figure 8. Variation of the ratio of stress intensity factors in couple-stress elasticity and in classical elasticity with ℓ/ξ.

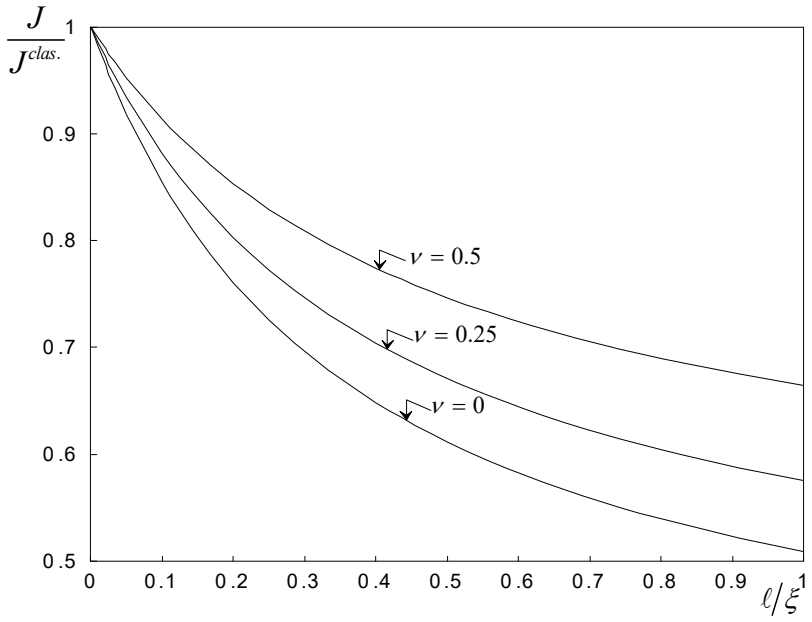

Figure 9. Variation of the ratio of the J -integrals in couple-stress elasticity and in classical elasticity with ℓ/ξ .

Figure 9 displays the dependence of the ratio $J/J^{clas.}$ upon the ratio of lengths ℓ/ξ. The quantity $J^{clas.} \equiv \tau_0^2\, \xi(1-\nu)/\mu$ is the integral provided by the classical elastic analysis. Contrary to the concentrated load case treated previously, the ratio $J/J^{clas.}$ decreases monotonically with increasing values of ℓ/ξ. A similar result was obtained in the case of a finite-length crack within the context of couple-stress [42] and dipolar gradient elasticity [30]. Finally, the ratio tends to the limit $1/(3-2\nu)$ as $\ell/\xi \to \infty$.

7. CONCLUDING REMARKS

In the present work, we examined the plane-strain problem of a semi-infinite crack under concentrated shear loading in a body with microstructure governed by couple-stress elasticity. The case of shear loading was chosen since, in principle, couple-stress effects are predominant in this type of deformation [9,17,41,42]. The case of a concentrated normal loading along the crack faces

will be treated in a future work. In general, solutions to problems with concentrated loads may serve as Green's functions for more general loadings.

The problem has two characteristic lengths, i.e. the length ℓ representing the material microstructure and the distance L between the point of application of the force and the crack-tip. Moreover, the problem involves stress concentration due to both loading and geometry (crack). The solution procedure was based on the two-sided Laplace transforms and on an analytic-function technique. For comparison purposes, the case of a semi-infinite crack subjected to an exponentially decaying shear load was also treated in the present study.

The results for the near-tip field in the concentrated load case showed some interesting features not encountered in previous investigations concerning finite-length or semi-infinite cracks under remote or distributed loading, within the framework of generalized continuum theories. More specifically, it was shown that the ratio of the stress intensity factors $K_{II}/K_{II}^{clas.}$ exhibits a bounded maximum within the range $0.2 \le \ell/L \le 0.25$ depending on the Poisson's ratio. This result is in contrast to the case of a semi-infinite crack with exponentially decaying shearing tractions (treated in Section 6 of the paper), where the respective ratio decreased monotonically with increasing values of the ratio of the material length ℓ over the load-induced length ξ. It is worth noting, that in the latter case the ratio $K_{II}/K_{II}^{clas.}$ attains its maximum when $\ell \to 0$. A similar behavior was also observed in the case of central traction-free crack under remote shear loading [41].

As regards now the energy release rate, we have found that the ratio $J/J^{clas.}$ tends to unity when the couple-stress parameter ℓ tends to zero. Thus, the transition to the classical theory is continuous as far as the energy release rate is concerned (contrary to the behavior of the stress intensity factor noticed before). For $\ell \neq 0$, the ratio increases is with increasing values of ℓ/L attaining its maximum in the range $0.2 \le \ell/L \le 0.3$. The latter behavior is in marked contrast with the distributed load case and the previously investigated cases by Atkinson and Leppington [40], and by Gourgiotis and Georgiadis [30,42], where it was found that $J/J^{clas.}$ diminished monotonically being always *smaller* than unity. The different solution behavior in the concentrated load case may be attributed to the fact that it involves both load-induced and crack-induced stress concentrations.

Acknowledgement

The research leading to these results has received funding from the European Research Council under the European Community's Seventh Framework Programme (FP7/2007-2013) / ERC grant agreement n° 228051.

APPENDIX A

According to (69) the kernel $N(p)$ is given by the expression

$$N(p)=\frac{4(1-\nu)\ell^2p^2}{(3-2\nu)}+\frac{\left(1-4(1-\nu)\ell^2p^2\right)}{(3-2\nu)}\frac{\gamma}{\beta}\ . \tag{A1}$$

Further, for p real and $\varepsilon<|p|\le a$, the real and imaginary parts of $N(p)$ are

$$\mathrm{Re}\,N(p)=\frac{4(1-\nu)\ell^2p^2}{(3-2\nu)}\ ,\qquad \mathrm{Im}\,N(p)=\frac{\left(1-4(1-\nu)\ell^2p^2\right)}{(3-2\nu)}\frac{|\gamma|}{|\beta|}\,, \tag{A2}$$

where $|\gamma|=\left|a^2-p^2\right|^{1/2}$ and $|\beta|=\left|\varepsilon^2-p^2\right|^{1/2}$.

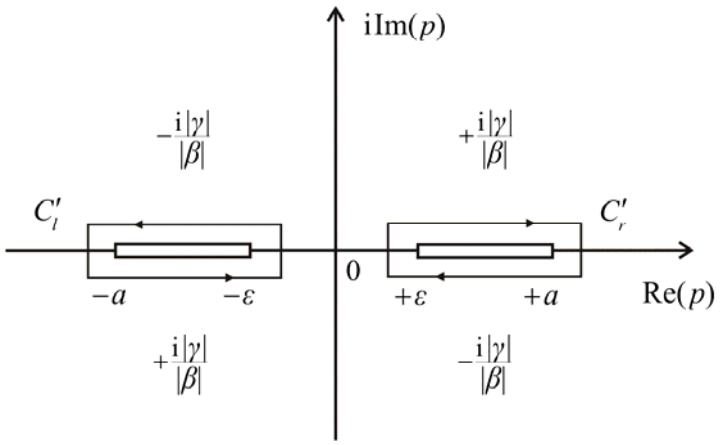

Figure A.1. Integration paths for the evaluation of the functions $N^{\pm}(p)$.

In order to determine the functions $N^{+}(p)$ and $N^{-}(p)$ defined in Eqs. (74), we close the integration paths C_r and C_l with large semi-circles at infinity on the right and left half-plane respectively, as it is shown in Fig. 3. Next, an alteration of the integration contour along with the use

of Cauchy's theorem and Jordan's Lemma, allows taking as equivalent integration paths the contours C_l' and C_r', around the branch cuts of $N(p)$ (see Fig. A.1).

In particular, for the function $N^+(p)$ we have

$$N^+(p) = \exp\left\{-\frac{1}{2\pi\mathrm{i}}\left(\int_{C_l'}\frac{\ln N(\zeta)}{\zeta-p}d\zeta\right)\right\}$$

$$= \exp\left\{-\frac{1}{2\pi\mathrm{i}}\left(\int_{-a}^{-\varepsilon}\frac{\ln N(\zeta)}{\zeta-p}d\zeta+\int_{-\varepsilon}^{-a}\frac{\ln N(\zeta)}{\zeta-p}d\zeta\right)\right\}$$

$$= \exp\left\{-\frac{1}{2\pi\mathrm{i}}\left(\int_{-a}^{-\varepsilon}\mathrm{i}\tan^{-1}\left[\frac{\mathrm{Im}\,N(\zeta)}{\mathrm{Re}\,N(\zeta)}\right]\frac{d\zeta}{\zeta-p}+\int_{-\varepsilon}^{-a}\mathrm{i}\tan^{-1}\left[\frac{-\mathrm{Im}\,N(\zeta)}{\mathrm{Re}\,N(\zeta)}\right]\frac{d\zeta}{\zeta-p}\right)\right\}$$

$$= \exp\left\{-\frac{1}{2\pi\mathrm{i}}\left(\int_{-a}^{-\varepsilon}(+\mathrm{i})\tan^{-1}\left[\frac{\left(1-4(1-\nu)\ell^2\zeta^2\right)}{4(1-\nu)\ell^2\zeta^2}\cdot\frac{\left|a^2-\zeta^2\right|^{1/2}}{\left|\varepsilon^2-\zeta^2\right|^{1/2}}\right]\frac{d\zeta}{\zeta-p}\right.\right.$$

$$\left.\left.+\int_{-\varepsilon}^{-a}(-\mathrm{i})\tan^{-1}\left[\frac{\left(1-4(1-\nu)\ell^2\zeta^2\right)}{4(1-\nu)\ell^2\zeta^2}\cdot\frac{\left|a^2-\zeta^2\right|^{1/2}}{\left|\varepsilon^2-\zeta^2\right|^{1/2}}\right]\frac{d\zeta}{\zeta-p}\right)\right\}$$

$$= \exp\left\{\frac{1}{\pi}\left(\int_0^a\tan^{-1}\left[\frac{\left(1-4(1-\nu)\ell^2\zeta^2\right)}{4(1-\nu)\ell^2\zeta^2}\cdot\frac{\left(a^2-\zeta^2\right)^{1/2}}{\left(\zeta^2-\varepsilon^2\right)^{1/2}}\right]\frac{d\zeta}{\zeta+p}\right)\right\}. \qquad \text{(A3)}$$

Similarly, integrating along C_r', we can evaluate the function $N^-(p)$. Finally, letting $\varepsilon\to 0$ and recalling that $a = 1/\ell$, we obtain

$$N^\pm \equiv N^\pm(p) = \exp\left\{\frac{1}{\pi}\left(\int_0^a\tan^{-1}\left[\frac{\left(1-4(1-\nu)\ell^2\zeta^2\right)}{4(1-\nu)\ell^3}\cdot\frac{\left(1-\ell^2\zeta^2\right)^{1/2}}{\zeta^3}\right]\frac{d\zeta}{\zeta\pm p}\right)\right\}. \qquad \text{(A4)}$$

APPENDIX B

For the evaluation of the integral in (89)

$$\frac{1}{2\pi \mathrm{i}} I = \frac{1}{2\pi \mathrm{i}} \int_{-\mathrm{i}\infty}^{\mathrm{i}\infty} \frac{e^{L\omega} \left(a+\omega\right)^{1/2} d\omega}{N^{+}\left(\omega\right)\left(\omega - p\right)} \,, \tag{B1}$$

that enters Eq. (84), we expand the integration path in the left half-plane $\left(\mathrm{Re}\,\omega < 0\right)$, as is shown in Fig. B.1.

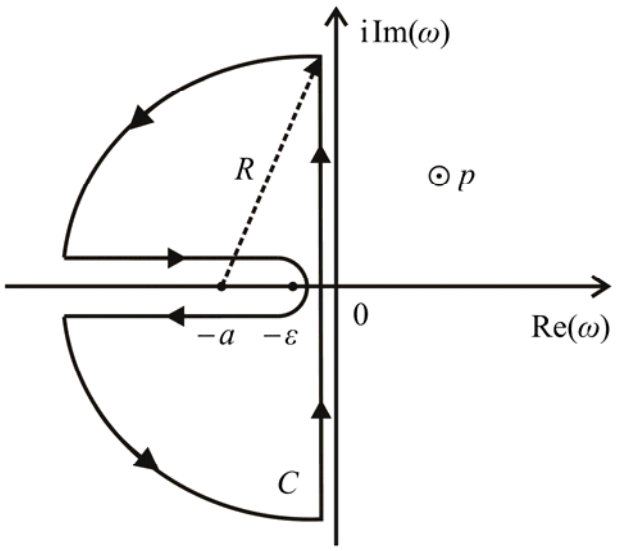

Figure B.1. The integration contour used for the evaluation of the integral I in the complex plane.

Considering the relation $N^{+}\left(p\right) = N\left(p\right) / N^{-}\left(p\right)$ and that $\lim_{|p|\to\infty} N^{+}\left(p\right) = 1$, the integral I is written by Cauchy's theorem as

$$\frac{1}{2\pi\mathrm{i}}I=-\frac{1}{2\pi\mathrm{i}}\left\{\lim_{R\to\infty}\left[\mathrm{i}\,R^{1/2}\int_{\pi/2}^{\pi}\exp\left(\mathrm{i}\frac{\theta}{2}+L\left(Re^{\mathrm{i}\theta}-a\right)\right)d\theta\right]+\int_{-\infty}^{-a}\frac{+\mathrm{i}\left|a+\omega\right|^{1/2}e^{L\omega}}{N^{+}(\omega)(\omega-p)}d\omega\right.$$

$$+\int_{-a}^{-\varepsilon}\frac{\left|a+\omega\right|^{1/2}N^{-}(\omega)e^{L\omega}}{\left[\mathrm{Re}\,N(\omega)-\mathrm{i}\,\mathrm{Im}\,N(\omega)\right](\omega-p)}d\omega+\int_{-\varepsilon}^{-a}\frac{\left|a+\omega\right|^{1/2}N^{-}(\omega)e^{L\omega}}{\left[\mathrm{Re}\,N(\omega)+\mathrm{i}\,\mathrm{Im}\,N(\omega)\right](\omega-p)}d\omega$$

$$\left.+\int_{-a}^{-\infty}\frac{-\mathrm{i}\left|a+\omega\right|^{1/2}e^{L\omega}}{N^{+}(\omega)(\omega-p)}d\omega+\lim_{R\to\infty}\left[\mathrm{i}\,R^{1/2}\int_{-\pi}^{-\pi/2}\exp\left(\mathrm{i}\frac{\theta}{2}+L\left(Re^{\mathrm{i}\theta}-a\right)\right)d\theta\right]\right\}, \quad \text{(B2)}$$

where R is the radius of the two quarter-circular paths having a center at point $p=-a$ (see Fig. B.1) and the angle θ $(-\pi\le\theta<\pi)$ is defined by the relation $p+a=R\,\mathrm{e}^{\mathrm{i}\theta}$. In view of the above, it follows that

$$\frac{1}{2\pi\mathrm{i}}I=\frac{1}{\pi}\left\{\int_{0}^{a}\frac{f(\omega)}{(\omega+p)}d\omega+\int_{a}^{\infty}\frac{h(\omega)}{(\omega+p)}d\omega-\right.$$

$$\left.-\lim_{R\to\infty}\left[R^{1/2}e^{-La}\int_{\pi/2}^{\pi}\exp\left(RL\cos\theta\right)\cos\left(\frac{\theta}{2}+RL\sin\theta\right)d\theta\right]\right\}, \quad \text{(B3)}$$

where

$$f(\omega)=\frac{N^{+}(\omega)\left[\mathrm{Im}\,N(\omega)\right]\left|a-\omega\right|^{1/2}e^{-L\omega}}{\left[\mathrm{Re}\,N(\omega)\right]^{2}+\left[\mathrm{Im}\,N(\omega)\right]^{2}}\quad,\quad h(\omega)=\frac{\left|a-\omega\right|^{1/2}e^{-L\omega}}{N^{-}(\omega)}\ .$$

Now, it can be shown that the third integral inside the braces behaves as $O\left(R^{-1}\right)$ when $R\to\infty$, thus the limit of the last term in (B3) tends to zero.

In view of the above, the integral I takes finally the form

$$\frac{1}{2\pi\mathrm{i}}I=\frac{1}{\pi}\left[\int_{0}^{a}\frac{f(\omega)}{(\omega+p)}d\omega+\int_{a}^{\infty}\frac{h(\omega)}{(\omega+p)}d\omega\right]\equiv\frac{1}{\pi}G(p)\ . \quad \text{(B4)}$$

REFERENCES

[1] Cauchy, A.L. Note sur l' equilibre et les mouvements vibratoires des corps solides. *Comptes Rendus Acad. Sci.* Paris 32, 323-326 (1851).

[2] Voigt, W. Theoretische Studien uber die Elastizitatsverhaltnisse der Krystalle. *Abhandlungen der Königlichen Gesellschaft der Wissenschaften zu Göttingen*, 34, 3-51 (1887).

[3] Cosserat, E. and Cosserat, F. *Theorie des Corps Deformables*, Hermann et Fils, Paris, 1909.

[4] Toupin, R.A. Perfectly elastic materials with couple stresses. *Archive for Rational Mechanics and Analysis*, 11, 385-414 (1962).

[5] Mindlin, R.D. and Tiersten, H.F. Effects of couple-stresses in linear elasticity. *Archive for Rational Mechanics and Analysis*, 11, 415-448 (1962).

[6] Koiter, W.T. Couple-stresses in the theory of elasticity. Parts I and II. *Proceedings of the Koninklijke Nederlandse Akademie van Wetenschappen*, B67, 17-44 (1964).

[7] Mindlin, R.D. Influence of couple stresses on stress concentrations. *Experimental Mechanics*, 3, 1-7 (1963).

[8] Weitsman, Y. Couple-stress effects on stress concentration around a cylindrical inclusion in a field of uniaxial tension. *ASME Journal of Applied Mechanics*, 32, 424-428 (1965).

[9] Bogy, D.B. and Sternberg, E. The effect of couple-stresses on singularities due to discontinuous loadings. *International Journal of Solids and Structures*, 3, 757-770 (1967).

[10] Lakes, R.S. *Experimental methods for study of Cosserat elastic solids and other generalized continua*. In: Mühlhaus H.-B. (Ed.), Continuum Models for Materials with Microstructure, Wiley & Sons, Chichester, 1-22, 1995.

[11] Maugin, G.A., 2010. Mechanics of generalized continua: What do we mean by that? In: Maugin G.A. and Metrikine A.V. (Eds.) Mechanics of Generalized Continua. One Hundred Years After the Cosserats. *Advances in Mathematics and Mechanics* 21, 253-262 (2010).

[12] Batra, R.C. Saint-Venant's principle in linear elasticity with microstructure. *Journal of Elasticity*, 13, 165-173 (1983).

[13] Batra, R.C. and Hwang, J. Dynamic shear band development in dipolar thermoviscoplastic materials. *Computational Mechanics*, 14, 354-369 (1994).

[14] Fleck, N. A., Muller, G.M., Ashby, M.F. and Hutchinson, J.W. Strain gradient plasticity: Theory and experiment. *Acta Metallurgica et Materialia*, 42, 475–487 (1994).

[15] Vardoulakis, I. and Sulem, J. *Bifurcation Analysis in Geomechanics*, Blackie Academic and Professional (Chapman and Hall), London, 1995.

[16] Huang, Y., Zhang, L., Guo, T.F. and Hwang, K.C. Mixed mode near-tip fields for cracks in materials with strain-gradient effects. *Journal of the Mechanics and Physics of Solids*, 45, 439-465 (1997).

[17] Huang, Y., Chen, J.Y., Guo, T. F., Zhang, L. and Hwang, K.C. Analytic and numerical studies on mode I and mode II fracture in elastic-plastic materials with strain gradient effects. *International Journal of Fracture*, 100, 1-27 (1999).

[18] Zhang, L., Huang, Y., Chen, J.Y. and Hwang, K.C. The mode-III full-field solution in elastic materials with strain gradient effects. *International Journal of Fracture*, 92, 325-348 (1998).

[19] Lubarda, V.A. and Markenskoff, X. Conservation integrals in couple stress elasticity. *Journal of the Mechanics and Physics and Solids*, 48, 553-564 (2000).

[20] Georgiadis, H.G. and Velgaki, E.G. High-frequency Rayleigh waves in materials with microstructure and couple-stress effects. *International Journal of Solids and Structures*, 40, 2501-2520 (2003).

[21] Georgiadis, H.G. The Mode-III crack problem in microstructured solids governed by dipolar gradient elasticity: static and dynamic analysis. *ASME Journal of Applied Mechanics*, 70, 517-530 (2003).

[22] Radi, E. and Gei, M. Mode III crack growth in linear hardening materials with strain gradient effects. *International Journal of Fracture*, 130, 765-785 (2004).

[23] Polyzos, D., Tsepoura, K.G. and Beskos, D.E. Transient dynamic analysis of 3-D gradient elastic solids by BEM. *Computers and Structures*, 83, 783-792 (2005).

[24] Lazar, M. and Maugin, G.A. Nonsingular stress and strain fields of dislocations and disclinations in first strain gradient elasticity. *International Journal of Engineering Science*, 43, 1157-1184 (2005).

[25] Grentzelou, C.G. and Georgiadis, H.G. Uniqueness for plane crack problems in dipolar gradient elasticity and in couple-stress elasticity. *International Journal of Solids and Structures*, 42, 6226-6244 (2005).

[26] Grentzelou, C.G. and Georgiadis, H.G. Balance laws and energy release rates for cracks in dipolar gradient elasticity. *International Journal of Solids and Structures*, 45, 551-567 (2008).

[27] Georgiadis, H.G. and Grentzelou, C.G. Energy theorems and the *J*-integral in dipolar gradient elasticity. *International Journal of Solids and Structures*, 43, 5690-5712 (2006).

[28] Tsamasphyros, G.I., Markolefas, S. and Tsouvalas, D.A. Convergence and performance of the h- and p-extensions with mixed finite element C^0-continuity formulations, for tension and

buckling of a gradient elastic beam. *International Journal of Solids and Structures*, 44, 5056-5074 (2007).

[29] Giannakopoulos, A.E. and Stamoulis, K. Structural analysis of gradient elastic components. *International Journal of Solids and Structures*, 44, 3440-3451 (2007).

[30] Gourgiotis, P.A. and Georgiadis, H.G. Plane-strain crack problems in microstructured solids governed by dipolar gradient elasticity. *Journal of the Mechanics and Physics of Solids*, 57, 1898-1920 (2009).

[31] Aravas, N. and Giannakopoulos, A.E. Plane asymptotic crack-tip solutions in gradient elasticity. *International Journal of Solids and Structures*, 46, 4478-4503 (2009).

[32] Gourgiotis, P.A., Sifnaiou, M.D. and Georgiadis, H.G. The problem of sharp notch in microstructured solids governed by dipolar gradient elasticity. *International Journal of Fracture*, 166, 179-201 (2010).

[33] dell'Isola, F., Sciarra, G. and Vidoli, S. Generalized Hooke's law for isotropic second gradient materials. *Proceedings of the Royal Society A: Mathematical, Physical and Engineering Sciences*, 465, 2177-2196 (2009).

[34] Chen, J.Y., Huang, Y. and Ortiz, M. Fracture analysis of cellular materials: a strain gradient Model. *Journal of the Mechanics and Physics of Solids*, 46, 789-828 (1998).

[35] Chang, C.S., Shi, Q. and Liao, C.L. Elastic constants for granular materials modeled as first-order strain-gradient continua. *International Journal of Solids and Structures*, 40, 5565-5582 (2003).

[36] Lakes, R.S. Size effects and micromechanics of a porous solid. *Journal of the Materials Science*, 18, 2572-258 (1983).

[37] Lakes, R.S. Strongly Cosserat elastic lattice and foam materials for enhanced toughness. *Cellular Polymers*, 12, 17-30 (1993).

[38] Bigoni, D. and Drugan, W.J. Analytical derivation of Cosserat moduli via homogenization of heterogeneous elastic materials. *ASME Journal of Applied Mechanics*, 74, 741-753 (2007).

[39] Sternberg, E. and Muki, R. The effect of couple-stresses on the stress concentration around a crack. *International Journal of Solids and Structures*, 3, 69-95 (1967).

[40] Atkinson, C. and Leppington, F.G. The effect of couple stresses on the tip of a crack. *International Journal of Solids and Structures*, 13, 1103-1122 (1977).

[41] Gourgiotis, P.A. and Georgiadis, H.G. Distributed dislocation approach for cracks in couple-stress elasticity: shear modes. *International Journal of Fracture*, 147, 83-102 (2007).

[42] Gourgiotis, P.A. and Georgiadis, H.G. An approach based on distributed dislocations and disclinations for crack problems in couple-stress elasticity. *International Journal of Solids and Structures*, 45, 5521-5539 (2008).

[43] Shi, M.X., Huang, Y. and Hwang, K.C. Fracture in the higher-order elastic continuum. *Journal of the Mechanics and Physics of Solids*, 48, 2513-2538 (2000).

[44] Fleck, N.A., Hutchinson, J.W. Strain gradient plasticity. In: Hutchinson, J.W., Wu, T.Y. (Eds.), *Advances in Applied Mechanics*, Vol. 33, Academic Press, New York, 295-361. (1997)

[45] Chen, J.Y., Wei, Y., Huang, Y., Hutchinson, J.W. and Hwang, K.C. The crack tip fields in strain gradient plasticity: The asymptotic and numerical analyses. *Engineering Fracture Mechanics*, 64, 625-648 (1999).

[46] Wei, Y. A new finite element method for strain gradient theories and applications to fracture analyses. *European Journal of Mechanics A/Solids*, 25, 897-913 (2006).

[47] Gourgiotis, P.A. and Georgiadis, H.G. The problem of a sharp notch in couple-stress elasticity. *International Journal of Solids and Structures*, 48, 2630-2641 (2011).

[48] Georgiadis, H.G. and Brock, L.M. An exact method for cracked elastic strips under concentrated loads – Time-harmonic response. *International Journal of Fracture*, 63, 201-214 (1993).

[49] Aero, E.L. and Kuvshinskii, E.V. Fundamental equations of the theory of elastic media with rotationally interacting particles. *Fizika Tverdogo Tela*, 2, 1399–1409. Translated in *Soviet Physics – Solid State*, 2, 1272-1281 (1960).

[50] Palmov, V.A. The plane problem of non-symmetrical theory of elasticity. *Applied Mathematics and Mechanics (PMM)*, 28, 1117-1120 (1964).

[51] Muki, R. and Sternberg, E. The influence of couple-stresses on singular stress concentrations in elastic solids. *Journal of Applied Mathematics and Physics (ZAMP)*, 16, 611-618 (1965).

[52] Jaunzemis, W. *Continuum Mechanics*, McMillan, New York, 1967.

[53] Nowacki, W. *Theory of Asymmetric Elasticity*, Pergamon Press, 1986.

[54] Sciarra, G. and Vidoli, S. The role of edge forces in conservation laws and energy release rates of strain-gradient solids *Mathematics and Mechanics of Solids,* doi:10.1177/10812865114 10412 (2011).

[55] Van der Pol, B. and Bremmer, H. *Operational Calculus Based on the Two-Sided Laplace Integral*, Cambridge University Press, Cambridge, UK, 1950.

[56] Carrier, G.A., Krook M. and Pearson, C.E. *Functions of a Complex Variable*, McGraw-Hill, New York, 1966.

[57] Roos, B.W. *Analytic Functions and Distributions in Physics and Engineering*, John Wiley and Sons, New York, 1969.

[58] Mittra, R. and Lee, S.W. *Analytical Techniques in the Theory of Guided Waves*, MacMillan, New York, 1971.

[59] Gelfand, I.M. and Shilov, G.E. *Generalized Functions I*, Academic Press, New York, 1964.

[60] Misra, O.P. and Lavoine, J.L. *Transform Analysis of Generalized Functions*, North-Holland, 1986.

[61] Kaya, A.C. and Erdogan, F. On the solution of integral equations with strongly singular kernels. *Quarterly of Applied Mathematics*, XLV (1), 105-122 (1987).

[62] Paget, D.F. A quadrature rule for finite-part integrals. *BIT Numerical Mathematics*, 21, 212-220, (1981).

[63] Tada, H., Paris, P.C. and Irwin, G.R. *Stress Analysis of Cracks Handbook*, Del Research Corporation, Hellertown, PA, 1973.

[64] Atkinson, C. and Leppington, F.G. Some calculations of the energy-release rate G for cracks in micropolar and couple-stress elastic media. *International Journal of Fracture*, 10, 599-602 (1974).

[65] Maugin, G.A. On the structure of the theory of polar elasticity. *Philosophical Transactions of the Royal Society A*, 356, 1367-1395 (1998).

[66] Freund, L.B. Energy flux into the tip of an extending crack in an elastic solid. *Journal of Elasticity*, 2, 341-349 (1972).

[67] Burridge, R. An influence function of the intensity factor in tensile fracture. *International Journal of Engineering Science*, 14, 725-734 (1976).

[68] Fisher, B. The product of distributions. *Quarterly Journal of Mathematics*, Oxford 22, 291-298 (1971).

[69] Freund, L.B. Stress intensity factor calculations based on a conservation integral. *International Journal of Solids and Structures*, 14, 241-250 (1978).

[70] Barber, J.R. *Elasticity*, Kluwer Academic Publishers, Dordrecht, 2002.